Rapidly calculated DFT relaxed iso-potential maps: β-cellobiose

ARTICLE *in* CELLULOSE · AUGUST 2011

Impact Factor: 3.57 · DOI: 10.1007/s10570-011-9537-8

2 AUTHORS:

Udo Schnupf
United States Department of Agriculture
43 PUBLICATIONS **420** CITATIONS
SEE PROFILE

Frank A Momany
United States Department of Agriculture
122 PUBLICATIONS **6,977** CITATIONS
SEE PROFILE

Cellulose (2011) 18:859–887
DOI 10.1007/s10570-011-9537-8

Rapidly calculated DFT relaxed iso-potential ϕ/ψ maps: β-cellobiose

U. Schnupf · F. A. Momany

Received: 14 September 2010 / Accepted: 25 March 2011 / Published online: 16 April 2011

Abstract New cellobiose ϕ_H/ψ_H maps are generated using a mixed basis set DFTr method, found to achieve a high level of confidence while reducing computer resources dramatically. Relaxed iso-potential maps are created for different conformational states of cellobiose, showing how glycosidic bond dihedral angles vary as different sets of hydroxymethyl rotamers and hydroxyl directions are examined. These maps are generated, fixing the dihedral ϕ_H and ψ_H values at ten degree intervals and energy optimizing the remaining geometry using the B3LYP/6-31+G* functional for all atoms except carbon atoms, where the functional B3LYP was used with the mixed basis set, 4-31G. Mapping results are compared between in vacuo structures using the mixed basis set, in vacuo using the full basis set, and those in which the implicit solvent method, COSMO, is included with the mixed basis set. Results show significant changes in position of energy minima with variation in hydroxyl rotamers and with application of solvent. Unique to this study is the mapping of the hydration energy at each ϕ_H/ψ_H point on the map using the energy derived at each point by applying COSMO. Using hydration gradients as a guide one observes directional solvent driven changes in the minimum energy positions. Interesting internal coordinate variances are described.

Keywords Cellobiose · DFT · 6-31+G*/4-31G · Iso-potential maps · COSMO

Introduction

Internal coordinates and conformational maps of maltose, an $\alpha(1 \rightarrow 4)$-linked disaccharide (Schnupf et al. 2007) and optimized structures of cellobiose, a $\beta(1 \rightarrow 4)$-linked disaccharide (Strati et al. 2002a, b; Chen and Naidoo 2003; Bosma et al. 2006a, b; French and Johnson 2008), have been studied by density functional (DFT) computational methods. A "Mini Review" (Homans 1993) covered the conformational and dynamics of oligosaccharides up to 1993, and these early works will not be expanded upon here. Post 1993, empirical potential studies using molecular mechanics software, as well as some hybrid QM:MM, Hartree–Fock (HF), and DFT computational methods have been applied to cellobiose

Names are necessary to report factually on available data; however, the USDA neither guarantees nor warrants the standard of the product, and the use of the name by USDA implies no approval of the product to the exclusion of others that may also be suitable.

U. Schnupf
Department of Food Science, Cornell University, Ithaca, NY 14853, USA
e-mail: us33@cornell.edu

F. A. Momany (✉)
Plant Polymer Research, USDA, ARS, National Center for Agricultural Utilization Research, 1815 N. University St., Peoria, IL 61604, USA
e-mail: frank.momany@ars.usda.gov

[Shen et al. 2009 (AMBER/GLYCAM); Johnson et al. 2009 (QM:MM); Stortz and French 2008 (MM3); Pereira et al. 2006 (GROMOS); French and Johnson 2006 (HF/DFT); French and Johnson 2004 (HF/DFT); Stortz and Cerezo 2002; Umemura et al. 2003a, b (OPLS); Mendonca et al. 2002 (MM3); French et al. 2001 (HF); Asensio and Jimenez-Barbero 1995 (AMBER); French and Dowd 1993 (MM3); Peters et al. 1993 (MM2CARB/AMBER)]. Many different empirical force fields were compared using cellobiose as the model (Stortz et al. 2009), with minimum energy positions plotted on a map of dihedral ϕ/ψ angles. This map showed (Stortz et al. 2009) a large range of minimum energy positions on the map depending on the force field used, with some clusters forming in two distinct regions of conformational space. Another empirical method used constrained dynamics of rigid residues (York and Yi 2004) to map out cellobiose conformations.

With all of the previous published work available, one must ask why add to the mapping of the low-energy conformations of cellobiose. There are several important reasons for this. First, in this study, newly tested, rapidly calculated, DFT optimization methods are applied to map the energy versus glycosidic bond dihedral angles of cellobiose for all hydroxymethyl and hydroxyl conformers. Maps at this level of theory and geometry optimized at every point have not been published. Second, these calculations include a very widely and successfully used implicit solvation method, COSMO (Klamt and Schüürmann 1993) that allows the preparation of ϕ_H/ψ_H versus relative hydration energy maps, never previously published for cellobiose. This application of COSMO is consistent with previous work (Tvaroska 1984; Kirschner and Woods 2001) in which solvent interactions were shown to be important in determining carbohydrate conformations and as found here, where significant shifts in the in vacuo minimum energy conformations result from addition of solvent to the maps. Advances in computing power, memory allotments, and advanced software have made it possible to examine such molecules at a high level of DFT theory while including a solvation model.

Relaxed iso-potential maps, often called Ramachandran plots, show regions of low energy as a function of incremental rotation about the glycosidic dihedral angles, ϕ/ψ, (ϕ_H/ψ_H when defined using the H1′–C1′–O4–C4 and H4–C4–O4–C1′ atoms). Most previously published cellobiose (Stortz and French 2008; French and Johnson 2004, 2008) maps are shown as composite or often called adiabatic maps. That is, they are the total of all the conformations studied from individual maps, showing the lowest energy state at each particular set of dihedral angles on the map. There are no cellobiose ϕ/ψ maps in the literature that provide the effects of solvation on the DFT energy minimized low energy conformational space, although empirical MM3 and ESFF force fields were used on α-lactoside with solvent model GB/SA (Asensio et al. 1997), and an ab initio HF/6-31G* study using rigid geometry and a solvent model (da Silva and Nascimento 2004) was carried out on β-lactose. Maps constructed without solvation included are doubtful for comparison with solution data since recent studies have implicated solvation as being important in the conformational preference and populations of the cellobiose molecule (Bosma et al. 2006a, b; Umemura et al. 2003a, b, 2005; Kirschner and Woods 2001), and as will be described here, solvent does play a significant role in variation of relative energies and in moving some glycosidic minimum energy positions by significant amounts on the ϕ/ψ maps produced.

Density functional iso-potential relaxed maps of β-cellobiose are prepared, a map for each of the different hydroxyl and hydroxymethyl rotamer conformations presented in Table 1. Maps are generated by choosing points in ϕ_H/ψ_H space at which the molecule is to be energy optimized, in this work they are chosen to be every 10° with ranges covering the low energy regions found in previous optimization studies of cellobiose (Strati et al. 2002a, b; Bosma et al. 2006a, b) and new positions presented here. The grid size is larger than that used for α-maltose maps (Schnupf et al. 2007) since the β-linked glycosidic bridge exhibits a smoother energy gradient around the minimum energy positions than maltose. The speed of production of the maps was enhanced by approximately tenfold over that using the full DFT, by the use of a reduced basis set on the carbon atoms in conjunction with the B3LYP functional (B3LYP/4-31G), while maintaining the B3LYP/6-31+G* functional for all other atoms, thus preserving the hydrogen bonding abilities of the higher level DFT calculations. The production of these maps enhances our abilities in making more specific comparisons to experimental results (Wacowich-Sgarbi et al. 2001; Sivchik and Zhbankov 1977; Andrianov et al. 1980;

Table 1 Relative energies[a] of local minima, hydration energies, and the ϕ_H/ψ_H dihedral angles around the glycosidic bond at the minimum energy position

	Rel. energies (kcal/mol)			Hydration energy (kcal/mol)	ϕ_H/ψ_H Minima angles (degree)		
	Vacuo DFTr[b]	Vacuo 6-31+G*[c]	COSMO 6-31+G*[d]		Vacuo DFTr	Vacuo 6-31+G*	COSMO 6-31+G*
Syn form							
gg′(r)–gg(r)	4.7	4.5	2.3	−29.8	−27/−33	−30/−31	−31/−28
gg′(c)–gg(c)	5.6	5.5	3.5	−29.1	35/−16	35/−16	33/−22
gt′(r)–gt(r)	6.6	6.6	1.7	−32.3	38/−59	37/−59	38/−21
gt′(c)–gt(c)	8.2	7.7	4.0	−31.4	42/−12	43/−10	42/−9
tg′(r)–tg(r)	7.7	7.4	4.5	−30.1	14/−35	15/−37	12/−28
tg′(c)–tg(c)	5.3	5.1	2.2	−30.1	30/−25	30/−25	31/−24
gg′(r)–gt(r)	7.5	7.2	4.0	−30.3	28/−66	25/−62	21/−58
gg′(c)–gt(c)	6.3	6.2	3.3	−30.2	29/−27	31/−25	33/−23
gt′(r)–gg(r)	4.2	4.1	2.3	−29.8	−27/−33	−28/−31	−24/−31
gt′(c)–gg(c)	6.9	6.5	4.1	−31.4	43/−5	41/−8	41/−10
gg′(r)–tg(r)	7.6	7.4	4.2	−30.2	12/−34	11/−35	9/−31
gg′(c)–tg(c)	5.7	5.5	2.1	−30.7	28/−26	28/−26	28/−25
tg′(r)–gg(r)	4.7	4.6	2.6	−29.7	−24/−34	−16/−34	−17/−33
tg′(c)–gg(c)	5.2	5.0	3.6	−30.2	40/−4	38/−8	42/−16
tg′(r)–gt(r)	6.5	6.3	1.1	−31.4	40/−19	41/−15	38/−14
tg′(c)–gt(c)	6.0	5.9	3.3	−29.9	31/−25	31/−24	33/−23
gt′(r)–tg(r)	6.7	6.3	1.0	−32.0	27/−31	29/−32	29/−25
gt′(c)–tg(c)	7.9	7.4	3.2	−31.7	36/−14	37/−14	30/−13
ϕ_H–*Anti* form							
gg′(r)–gg(r)–ϕ_H–*anti*	0.0	0.0	0.0	−27.4	179/−1	180/0	180/0
gg′(c)–gg(c)–ϕ_H–*anti*	2.4	2.3	3.5	−26.4	179/0	180/0	178/1
gt′(r)–gt(r)–ϕ_H–*anti*	3.4	3.6	1.9	−29.0	180/−4	175/−4	181/−4
gt′(c)–gt(c)–ϕ_H–*anti*	8.6	8.4	5.4	−30.5	178/−6	178/−6	178/−4
tg′(r)–tg(r)–ϕ_H–*anti*	2.5	2.6	2.0	−27.9	178/−2	178/−2	178/−2
tg′(c)–tg(c)–ϕ_H–*anti*	7.1	7.2	5.3	−29.1	180/−5	180/−4	181/−2
ψ_H–*Anti* form							
gg′(r)–gg(r)–ψ_H–*anti*	7.0	6.5	4.1	−29.7	12/181	12/180	11/179
gg′(c)–gg(c)–ψ_H–*anti*	8.8	8.2	5.8	−29.8	13/182	12/182	10/182
gt′(r)–gt(r)–ψ_H–*anti*	8.8	8.8	5.1	−30.4	57/209	57/209	6/177
gt′(c)–gt(c)–ψ_H–*anti*	7.9	7.4	5.2	−30.3	32/173	31/173	27/176
tg′(r)–tg(r)–ψ_H–*anti*	5.9	5.7	6.4	−26.5	2/180	3/181	6/184
tg′(c)–tg(c)–ψ_H–*anti*	8.3	8.1	6.4	−28.8	4/181	4/182	6/182
Anti–anti form							
gg′(r)–gg(r)–*anti–anti*	16.2	15.6	11.4	−31.2	179/215	178/213	201/189
gg′(c)–gg(c)–*anti–anti*	14.0	13.7	12.1	−29.3	186/201	185/201	185/200
gt′(r)–gt(r)–*anti–anti*	16.5	16.1	13.6	−30.4	173/191	174/191	173/192
gt′(c)–gt(c)–*anti–anti*	16.2	15.7	12.6	−30.1	189/201	188/197	182/202

Table 1 continued

	Rel. energies (kcal/mol)			Hydration energy (kcal/mol)	ϕ_H/ψ_H Minima angles (degree)		
	Vacuo DFTr[b]	Vacuo 6-31+G*[c]	COSMO 6-31+G*[d]		Vacuo DFTr	Vacuo 6-31+G*	COSMO 6-31+G*
tg′(r)–tg(r)–*anti*–*anti*	14.3	14.1	12.7	−28.9	178/198	182/199	183/197
tg′(c)–tg(c)–*anti*–*anti*	16.1	15.9	10.7	−32.8	189/196	188/197	186/200

[a] Relative energies with respect to overall lowest energy minimum: vacuo-DFTr −814,060.05 kcal/mol; vacuo 6-31+G* −814,487.69 kcal/mol, and COSMO/6-31+G* −814,515.02 kcal/mol, respectively

[b] Level of Theory B3LYP/6-31+G*(O,H)/4-31G(C) which is DFTr

[c] Level of theory B3LYP/6-31+G*//DFTr

[d] Level of Theory B3LYP/6-31+G*/COSMO//DFTr

Hamer et al. 1978; Horii et al. 1982, 1983; Korolik et al. 1985; Tvaroska and Taravel 1992; Duus et al. 1994; Sugiyama et al. 2000; Suzuki et al. 2009; Cheetham et al. 2003; Larsson et al. 2004; Olsson et al. 2008; Cocinero et al. 2009; Asensio and Jimenez-Barbero 1995; Chu and Jeffrey 1968) as will be described later.

Examination of previous DFT optimization studies on cellobiose (Strati et al. 2002a, b; Bosma et al. 2006a, b) showed that different rotamers of the hydroxymethyl groups influenced the conformational low energy regions at the glycosidic bonds. Further, in the case of α-maltose (Schnupf et al. 2007), the preferred low energy in vacuo conformations were 'c' forms, with the exception that upon application of the solvent method, COSMO, the 'r' form became energy preferred. In our previous cellobiose studies (Strati et al. 2002a, b; Bosma et al. 2006a, b), there was some question as to the lowest energy rotamer conformations and solvent dependence. Resolving the 'r' and 'c' question is of interest to us, but the observation that the ϕ_H–*anti* form was found to be the lowest energy conformation (Strati et al. 2002a) is contrary to experimental solution studies that indicated that the *syn* conformer is preferred (Hardy and Sarko 1993a, b; Wacowich-Sgarbi et al. 2001; Sivchik and Zhbankov 1977; Andrianov et al. 1980; Hamer et al. 1978; Horii et al. 1982, 1983; Korolik et al. 1985; Tvaroska and Taravel 1992; Duus et al. 1994; Sugiyama et al. 2000; Cheetham et al. 2003; Larsson et al. 2004; Olsson et al. 2008; Cocinero et al. 2009), and this must be resolved. Upon addition of explicit water molecules the *syn* conformation water complex does become of lower relative energy than the ϕ_H–*anti*-form (Bosma et al. 2006a, b) water complex, while application of COSMO during optimization did not show a complete shift to the *syn* form. However, recent DFTMD studies on cellobiose (Momany and Schnupf 2011) including the implicit solvent method, COSMO, showed that after 5 ps of dynamics, the *syn* form becomes lower in average free energy than the ϕ_H–*anti* form, suggesting that both solvent and entropy play a role in the solution structure of cellobiose. Addition of solvent moves different low energy conformers to new minima and changes in gradient can be seen on hydration energy maps. The novel inclusion of implicit hydration to these maps provides new insight into the solvation models of carbohydrates and shows clearly those conformations that are solvent preferred.

Computational method

As noted above, the functional form of the calculation is the B3LYP/6-31+G* functionals for all atoms except the carbon atoms, where B3LYP/4-31G functionals were used. This combination of basis sets (denoted DFTr) has been tested on a variety of carbohydrate examples (Schnupf et al. 2011) and found to be fully capable of providing high quality results, with only slight reduction in the accuracy of the relative energy differences, as compared with the use of the B3LYP/6-31+G* level on all the atoms. Several maps are presented using both the mixed DFTr (B3LYP/6-31+G*/4-31G) basis set and the complete DFT (B3LYP/6-31+G*) basis set as comparisons.

Parallel Quantum Solutions (PQS) software and hardware (QS16-2300S) were utilized throughout for the constrained energy optimization at each point on

the iso-potential ϕ_H/ψ_H map. Convergence criteria were similar to those used previously (Strati et al. 2002a, b; Bosma et al. 2006a, b; Schnupf et al. 2007) with energy change of less than 1×10^{-6} Hartree and gradient of less than 1×10^{-4} au. The new Hessians did not show negative eigenvalues after optimization, indicating each point is at a local minimum. Results are displayed using modeling tools (Hyperchem v8.0.2 (2007); ORIGIN v8.0 (2009)). Contour maps are created by interpolative methods between grid points. Clockwise, 'c', and counter-clockwise, 'r', conformational states of the hydroxyl groups are included, and combinations of the three hydroxymethyl conformers (gg, gt, tg), as well as the *syn* (H1′–C1′–O4–C4 = ϕ_H; C1′–O4–C4–H4 = ψ_H), *anti* (ϕ_H or ψ_H having a value of $\sim 180°$), and *anti–anti* conformations (both ϕ_H and ψ_H having a value of $\sim 180°$). Figure 1 presents the numbering scheme for the atoms, and conformations for the *syn*, ϕ_H–*anti*, ψ_H–*anti* and *anti–anti* forms.

The conformations studied, as noted above, include gg′–gg-r/c, gg′–gt-r/c, gg′–tg-r/c, gt′–gt-r/c, gt′–gg-r/c, gt′–tg-r/c, tg′–gg-r/c, tg′–gt-r/c, and tg′–tg-r/c. In several examples, in vacuo maps at both DFT levels of theory are directly compared. Conformers were calculated using the solvated reduced form, COSMO/B3LYP/6-31+G*//DFTr (denoted SolDFTr). Starting dihedral angles are chosen from tables of previous optimization studies (Strati et al. 2002a) and Table 1 with points taken at every 10° along the ϕ_H/ψ_H grid around the energy minimum chosen. To reduce the computational effort the maps are presented only around the minimum energy positions with the dihedral angles for the glycosidic bonds noted in Table 1. Upon incrementing the specific dihedral angle, the structure previously energy optimized in the array is used for the next starting structure. This method is useful in regions in which the energy gradients are reasonably smooth, the relative energy is small, and no major geometry changes occur between steps. Rings were checked for chair form at every point. Hydrogen (H1′ and H4) atoms were used to define the position of the constrained dihedral angles as discussed previously (Schnupf et al. 2007). Comparisons with crystallographic data (Ham and Williams 1970; Leung et al. 1976; Hirotsu and Shimada 1974; Peralta-Inga et al. 2002; Raymond et al. 1995; Gessler et al. 1995; Mackie et al. 2002) are made, but solution NMR results (Cheetham et al. 2003) are most directly comparable with calculations that include solvent.

Results and discussion

Table 1 lists the energies at the local energy minima (DFTr, 6-31+G*, 6-31+G*+COSMO, and the hydration energy) of all the conformations described here. The dihedral angles around the glycosidic bond at the minimum energy position are given. From Table 1 the differences in local minimum energy positions are found for the different DFT calculations. The maps described here use the ϕ_H/ψ_H notation throughout.

Presented in several figures are the relaxed (DFTr, full DFT, SolDFTr, and hydration energy) iso-potential maps for the conformations (gg′–gg-r/c, etc.) noted above. Further, shown in the figures is the molecular representation of cellobiose at its minimum energy conformation for the map of interest. Of interest is the difference between the in vacuo and solvated maps for each of the conformers, as well as the hydration relative energy map positioned alongside the SolDFTr total energy map. Beside the map differences presented from the different hydroxymethyl group rotamers, the energy minimum positions between the 'c' and 'r' secondary hydroxyl directions are also important. In the next sections the individual rotamer maps are presented, with all inclusive composite ("adiabatic") maps presented last.

gg′(r/c)–gg(r/c)

Figure 2a–d shows the relative energy maps for; in vacuo mixed basis, in vacuo and hydration by COSMO B3LYP/6-31+G* basis single point energy at mixed basis geometry, and the hydration energy maps, for gg′(r)–gg(r). The two maps in which the mixed basis and full basis are compared (Fig. 2a, b) appear very similar to the energy differences found in Table 1 between the optimized energies, with small deviations in relative energy between them, and this small difference is found for all the maps examined and optimized structures studied. Applying COSMO (Fig. 2c) lowers the optimized relative energy in Table 1 but moves the minimum energy position to

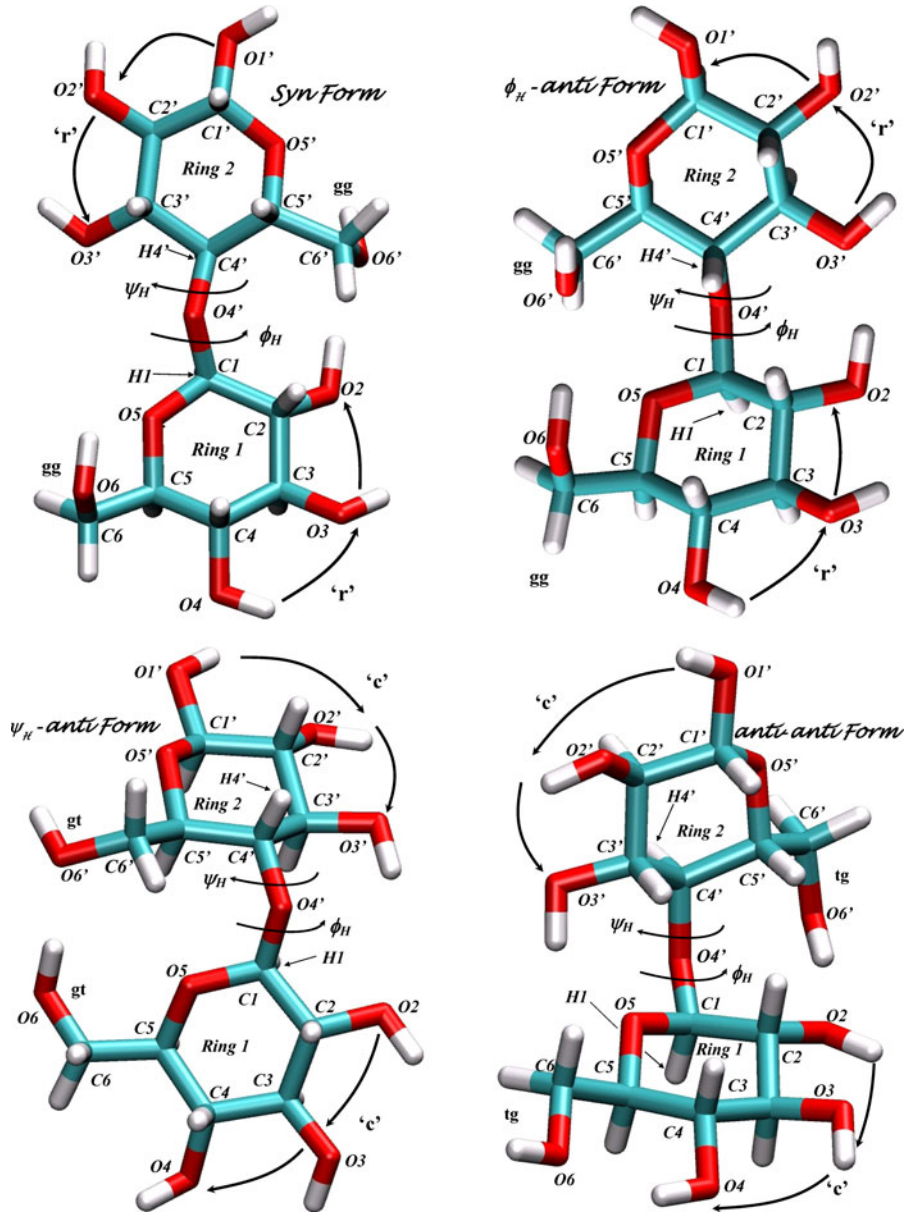

Fig. 1 Conformational states of cellobiose and numbering scheme

slightly smaller values in the ψ_H axis in the 'r' conformer. On the other hand, the hydration map (Fig. 2d) does not show that the minimum energy position is the most favorable by hydration energy. Rather, in the 'r' form the higher energy region around $\phi_H/\psi_H \sim 50°/-10°$ has a more negative energy of hydration than that around the energy minimum position. A secondary minimum that is higher in relative energy appears in the map at $\phi_H/\psi_H \sim 50°/25°$. This minimum is spread out in the hydration map broadly across $\sim 40°$ in the ϕ_H axis and is ~ 1.5 kcal/mol higher in relative energy than the minimum energy position. The average hydration energy over the complete map is -29.8 kcal/mol, while the effect of hydration is to drop the relative energy difference between the lowest energy form, gg′(r)–gg(r)–*ϕ*–*anti*, from ~ 4.5 kcal/mol for the vacuum case, to ~ 2.3 kcal/mol for the COSMO hydrated form. This change in the relative energy is important and confirms that solvent plays a

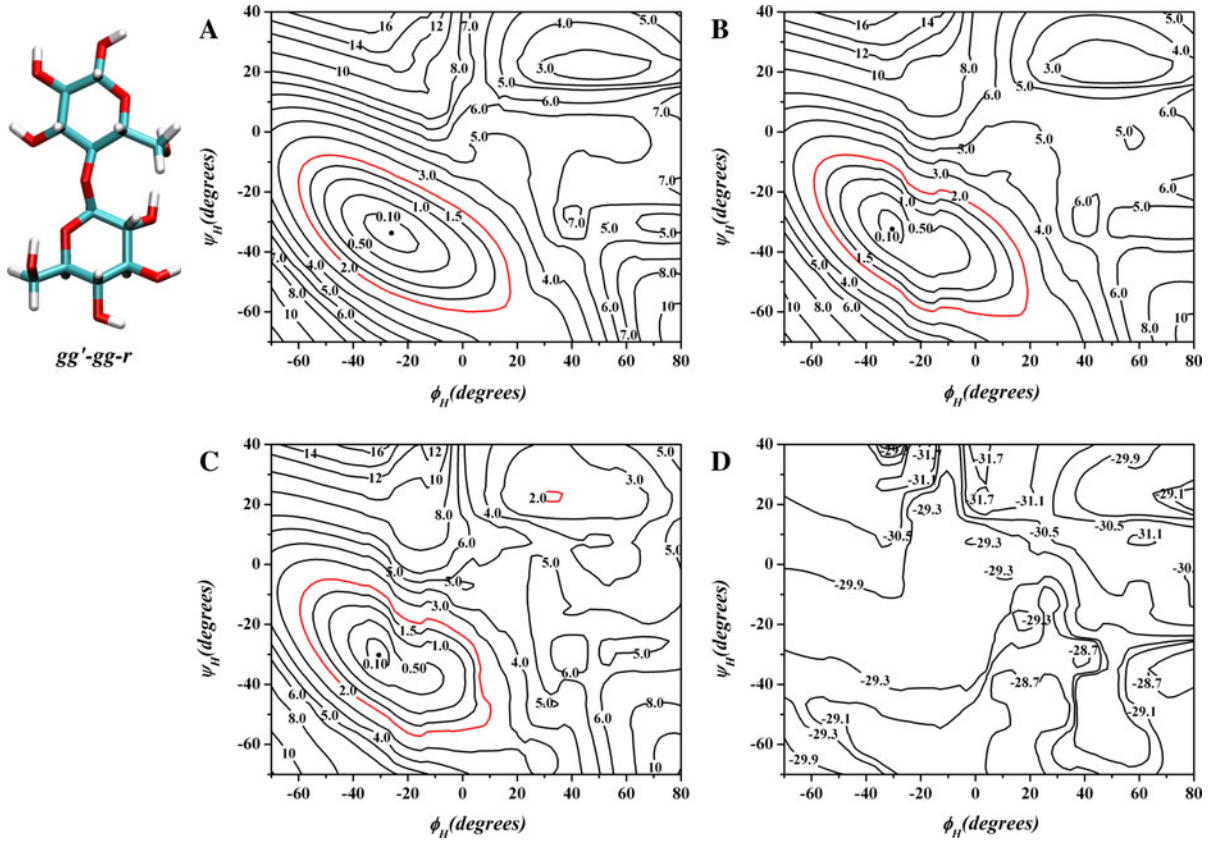

Fig. 2 Relaxed iso-potential (ϕ_H, ψ_H) maps for the gg′(r)–gg(r) conformations of β-cellobiose. The *contour lines* values are in kcal/mol and are relative to the lowest energy point. **a** E = −814,055.4 kcal/mol, DFTr in vacuo. **b** E = −814,483.183 kcal/mol B3LYP/6-31+G*//DFTr in vacuo. **c** E = −814,512.7 kcal/mol, SolDFTr. **d** COSMO hydration energy at the B3LYP/6-31+G*//DFTr level of theory

significant role in the stability of the *syn* conformation, as well as in changing the position of the energy minimum.

In Fig. 3a–d the four different gg′(c)–gg(c) maps produced from the conformational variation are shown. The 'c' or clockwise maps differ considerably from those of the 'r' or counterclockwise conformers. The 'c' map is much smoother overall than the 'r' form, with only slight differences in the position of the relative energy minimum as a response to solvation. The position of minimum energy is far removed from that of the 'r' form, suggesting that major conformational effects will result from these changes in hydroxyl positions. The hydration map does not have a minimum in the same position as the relative energy minimum although the negative values of the hydration energy are quite high at the minimum and increase in value as one goes to higher negative ψ_H values. The average hydration energy of −29.1 kcal/mol is for this conformation ∼0.7 kcal/mol less negative than was found for the 'r' form, suggesting that the 'r' form will be favored by solvation energy. The relative energy changes are similar to the 'r' form with the relative energy changing from ∼7.7 to ∼4.0 kcal/mol upon solvation, again a significant change resulting from solvation effects.

gg′(r/c)–gt(r/c)

Figure 4a–d shows energy and hydration values for the 'r' and 'c' forms of this conformer. Clearly placing the gt conformation at the reducing end creates a map that differs from the previous gg′–gg maps. Two energy minima appear in the 'r' conformer, the lowest energy being around ∼+27°/−70°

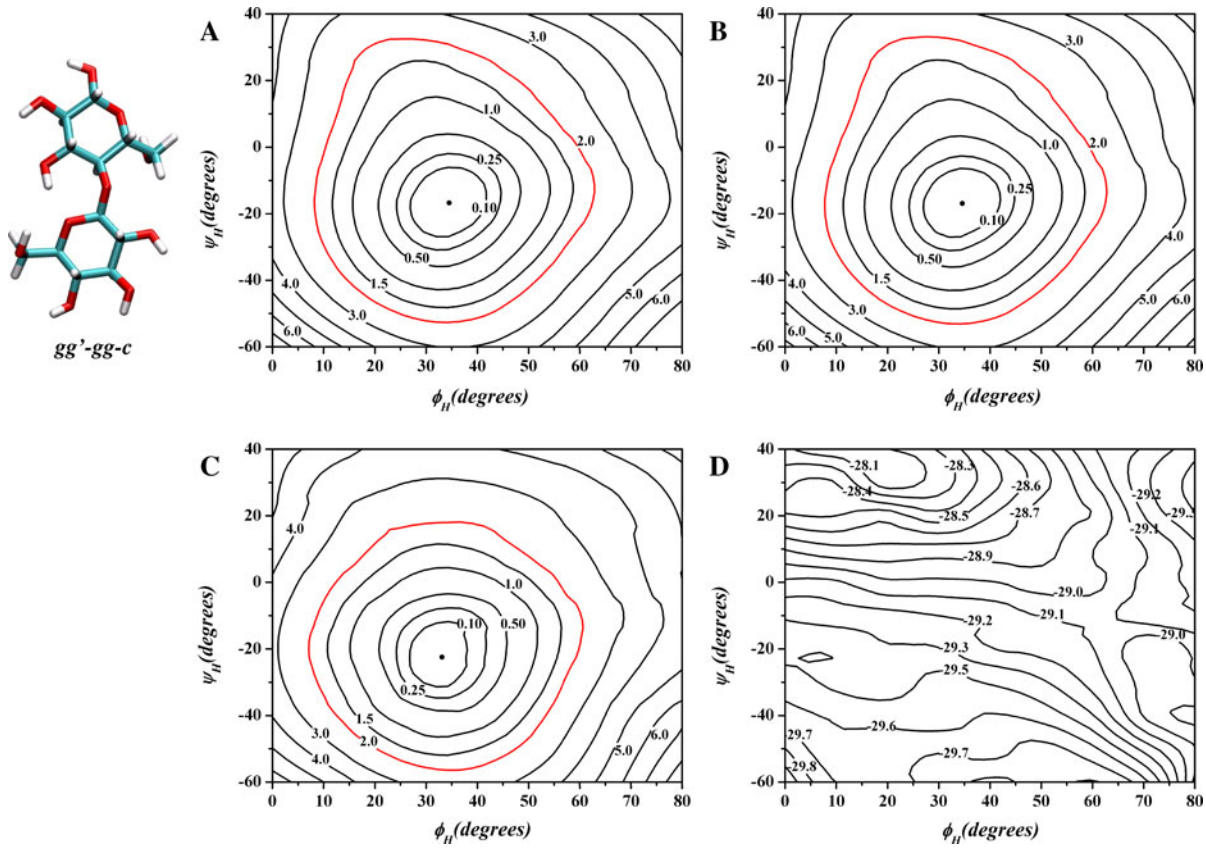

Fig. 3 Relaxed iso-potential (ϕ_H, ψ_H) maps for the gg′(c)–gg(c) conformations of β-cellobiose. The *contour lines* values are in kcal/mol and are relative to the lowest energy point. **a** E = −814,054.5 kcal/mol, DFTr in vacuo. **b** E = −814,482.156 kcal/mol B3LYP/6-31+G*//DFTr in vacuo. **c** E = −814,511.501 kcal/mol, SolDFTr. **d** COSMO hydration energy at the B3LYP/6-31+G*//DFTr level of theory

in ϕ_H/ψ_H while a second minimum appears at ∼+65°/0°. The energy barrier between the two minima is ∼2.5 kcal/mol in height relative to the lowest energy map point. The spread of energy points within the 1.0 kcal/mol. contour is very large, spanning over 40° in both ϕ_H and ψ_H and the slightly higher energy position, minimum two, spans about the same space, so for one map there is significant low energy space for this conformation to move without excessive change in energy. It is of interest to note that the mixing of the hydroxymethyl groups provides a reasonable low energy pathway between both the ψ_H–*anti* (i.e., more negative ψ_H direction) and the ϕ_H–*anti* (i.e., more positive ϕ_H values) forms. The reason for this is that mixed primary hydroxyl orientations are of higher energy which in turn lowers the energy barrier between the different *anti*-forms. By comparison, in the non-mixed hydroxymethyl orientations, there appears to be no low energy pathway between the different *anti*-forms. The hydration energy is nearly the same at both energy minima in Fig. 4a (see Fig. 4b).

Quite a different picture is found with the ‘c’ form as shown in Fig. 4c. The lowest energy position is ∼27°/−30° in ϕ_H/ψ_H. This is a normal position for an energy minimum in cellobiose. It should be noted that during the calculations a transition occurred at ϕ_H/ψ_H ∼ +30°/−83° providing a new low energy region. Upon examination of the conformation it was found that a new conformer was created, that is gg′(c)–gt(r) resulted from flipping all the hydroxyl groups on the reducing residue into the ‘r’ form and therefore was exclude from the map shown in Fig. 4c. The energy is ∼3.0 kcal/mol higher than the lowest

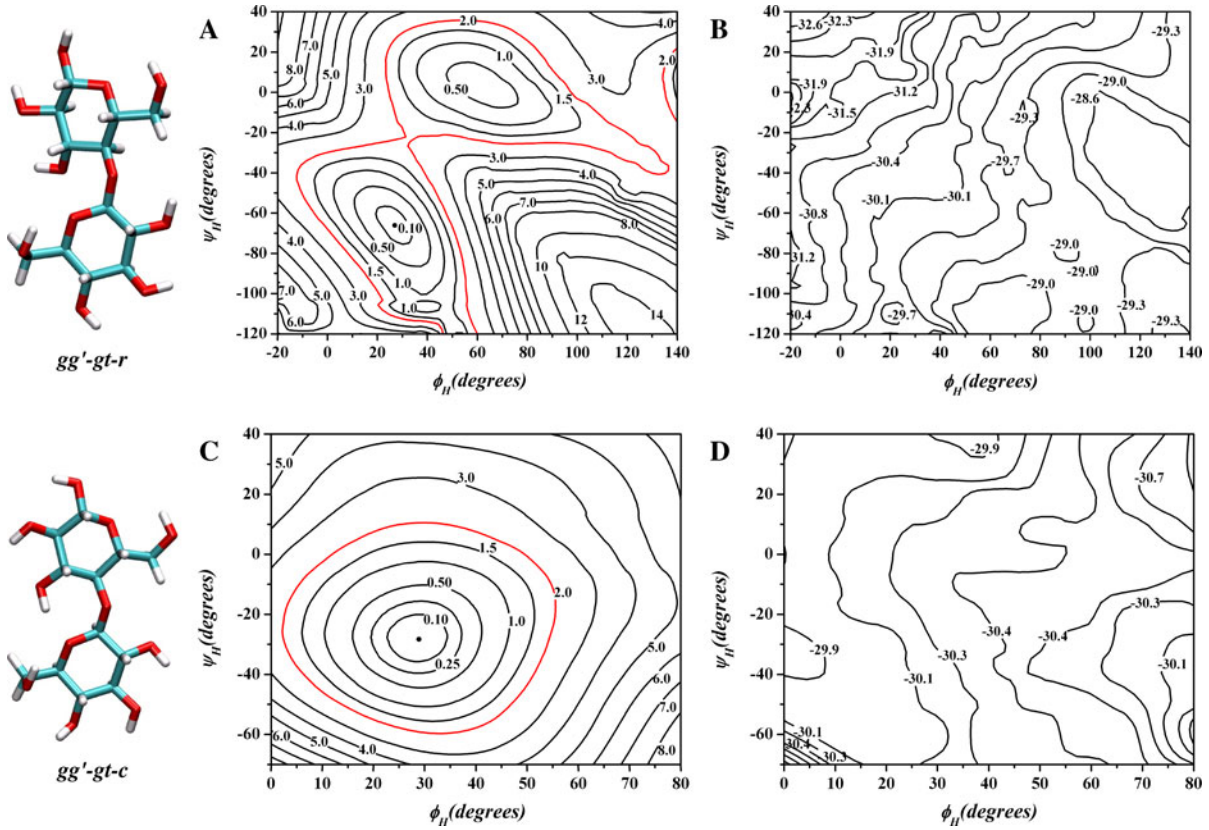

Fig. 4 Relaxed iso-potential (ϕ_H, ψ_H) maps for the gg′(r/c)–gt(r/c) conformations of β-cellobiose. The *contour lines* values are in kcal/mol and are relative to the lowest energy point. **a** gg′(r)–gt(r), E = −814,052.6 kcal/mol, DFTr in vacuo. **b** gg′(r)–gt(r), COSMO hydration energy at the B3LYP/6-31+G*//DFTr level of theory. **c** gg′(c)–gt(c), E = −814,053.8 kcal/mol, DFTr in vacuo using the mixed basis set geometry. **d** gg′(c)–gt(c), COSMO hydration energy at the B3LYP/6-31+G*//DFTr level of theory

energy position, but is a true minimum. The 'c' and 'r' hydration energies are very close at both energy minima.

gg′(r/c)–tg(r/c)

Figure 5a–d shows the 'r' and 'c' conformational energy and hydration maps for the gg′–tg hydroxymethyl groups. The 'r' map has one energy minimum with a broad spread of low energy encompassing almost 50° in ϕ_H and 30° in ψ_H to reach the 1.0 kcal/mol iso-potential curve. The 'c' form is similar in spread across the map, only shifted to ϕ_H/ψ_H values of ∼30°/−30°. A second local flat region (not shown) at ϕ_H/ψ_H ∼ 30°/−70° was found, a result of ring 2 flipping all hydroxyl groups to 'r'. The two hydration maps appear to be very different, particularly across the map at ψ_H ∼ 0°, but are closely comparable at the minimum energy positions.

gt′(r/c)–gt(r/c)

In Fig. 6a–d are shown the four figures for the gt′(r)–gt(r) form. In this conformational state, rather large variances in position of minimum occur when hydration is applied. The mixed basis and normal basis DFT results are again nearly identical, but when COSMO is applied, the minimum moved from ϕ_H/ψ_H ∼ 35°/−60° to a value of ϕ_H/ψ_H ∼ 35°/−20° or a ∼40° change in ψ_H to the minimum energy position, a result of the increase in negative energy arising from the hydration terms as seen in Fig. 6d. The average hydration energy for the gt′(r)–gt(r) conformation is −32.9 kcal/mol, considerably more

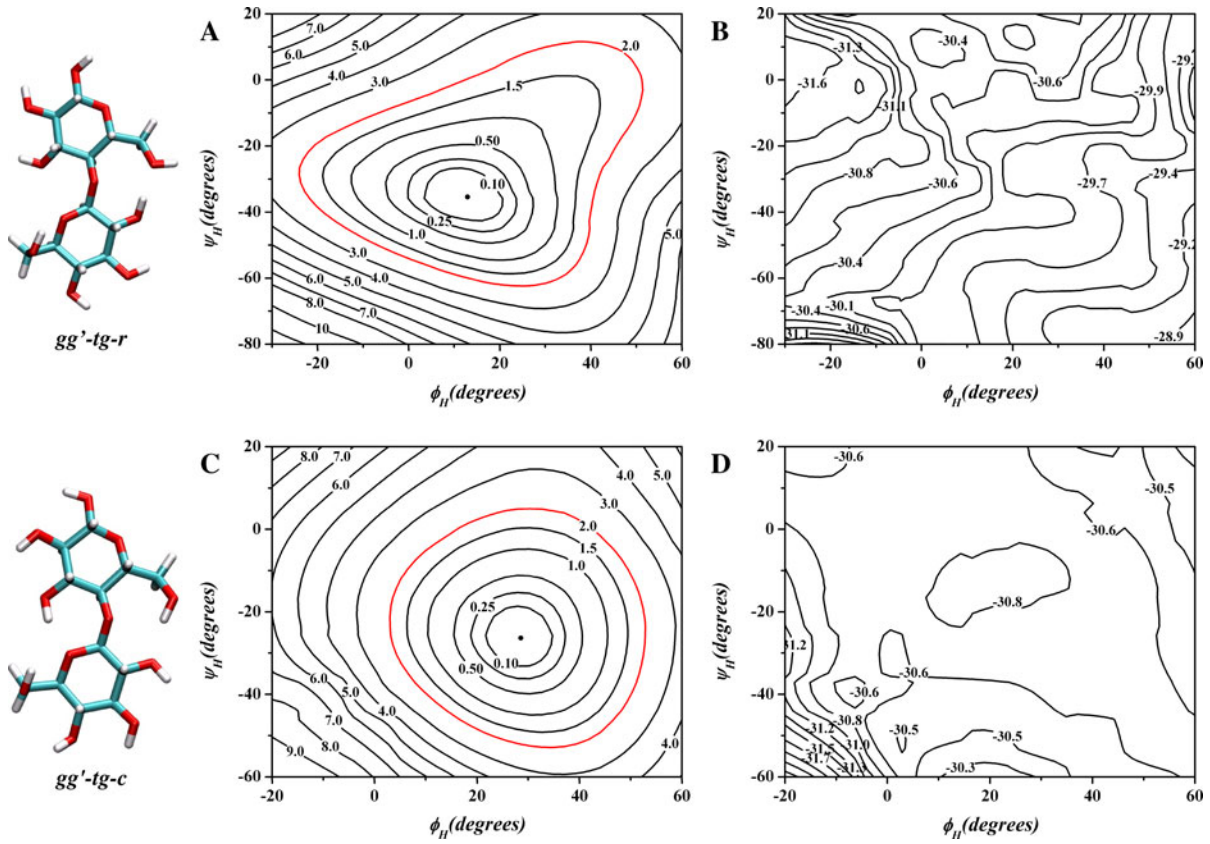

Fig. 5 Relaxed iso-potential (ϕ_H, ψ_H) maps for the gg′(r/c)–tg(r/c) conformations of β-cellobiose. The *contour lines* values are in kcal/mol and are relative to the lowest energy point. **a** gg′(r)–tg(r), E = −814,052.5 kcal/mol, DFTr in vacuo. **b** gg′(r)–tg(r), COSMO hydration energy at the B3LYP/6-31+G*//DFTr level of theory. **c** gg′(c)′tg(c), E = −814,054.4 kcal/mol, DFTr in vacuo using the mixed basis set geometry. **d** gg′(c)–tg(c), COSMO hydration energy at the B3LYP/6-31+G*//DFTr level of theory

negative than found for either of the gg′–gg forms and suggests that the gt′(r)–gt(r) conformations would be highly solvent favored. The total energy of this conformation is also the lowest relative energy (∼1.5 kcal/mol lower than the next best energy) in this series of conformers. It is of interest to note in Table 1 that the relative energies of the in vacuo studies are ∼6.5 kcal/mol while the solvation lowers the relative energy to ∼1.7 kcal/mol putting it in a much more favored condition when solvated.

Figure 7a–d shows results for gt′(c)–gt(c), and as found previously, the two in vacuo maps are very similar and the COSMO map shows some difference in the shape around the minimum energy position. The hydration map does not show large variances across the map in the region of the energy minimum, but reduces by ∼0.5–1.0 kcal/mol the height of the higher energy contours in the region of ϕ_H/ψ_H ∼ 70°/20°. The average hydration energy for this conformation is −31.4 kcal/mol. This value is not as negative as found for the ‘r’ form, but again suggests that the ‘r’ form will be favored by solvation. From Table 1 the relative energies for the in vacuo forms are ∼8.0 kcal/mol but are reduced upon solvation to ∼4.0 kcal/mol a significant change at the minimum energy position.

gt′(r/c)–gg(r/c)

Figure 8a–d shows both ‘r’ and ‘c’ forms maps for the gt′–gg hydroxymethyl conformation. The ‘c’ map has several minima, all around ∼30–40° in ϕ_H with the lowest energy around ψ_H ∼ −10°, a flat region at ∼−25° and a higher energy minimum at ∼−40°

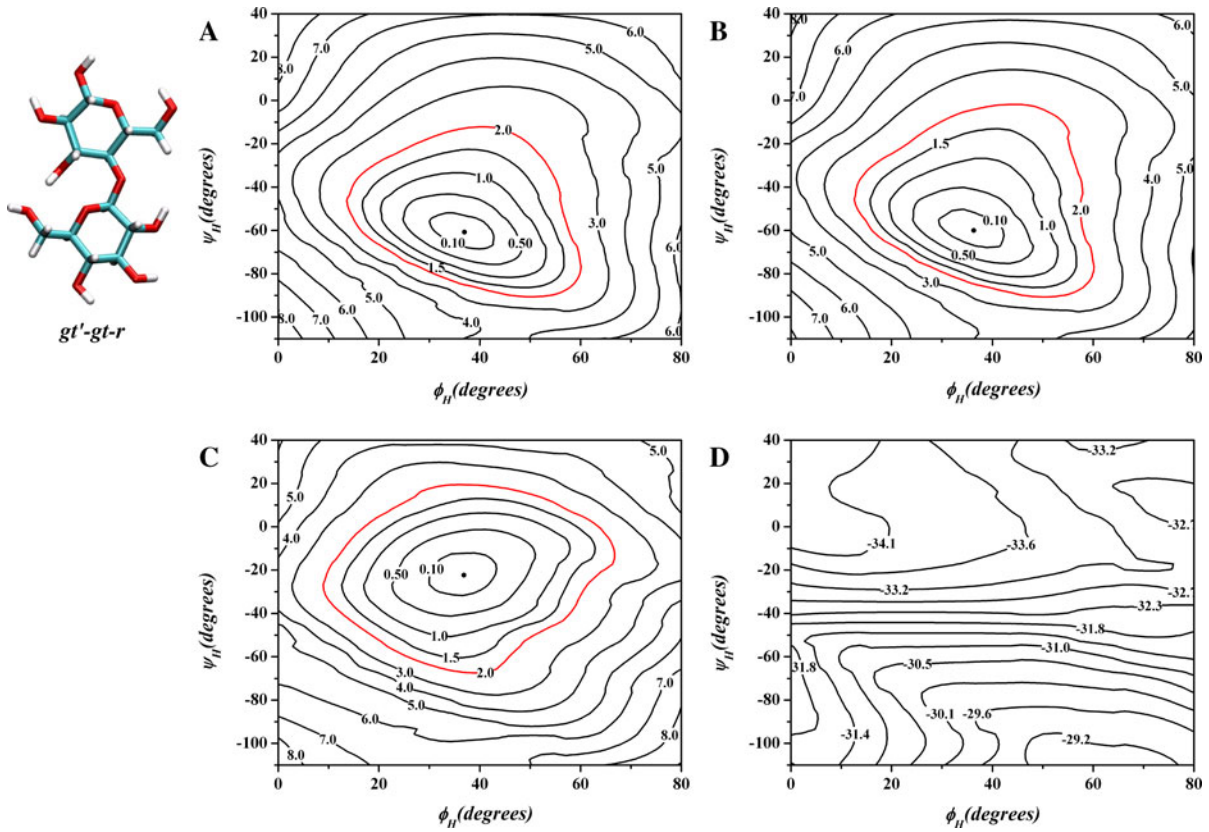

Fig. 6 Relaxed iso-potential (ϕ_H, ψ_H) maps the gt′(r)–gt(r) conformations of β-cellobiose. The *contour lines* values are in kcal/mol and are relative to the lowest energy point. **a** E = −814,053.5 kcal/mol, DFTr in vacuo. **b** E = −814,481.1 kcal/mol, B3LYP/6-31+G*//DFTr in vacuo. **c** E = −814,513.3 kcal/mol, SolDFTr. **d** COSMO hydration energy at the B3LYP/6-31+G*//DFTr level of theory

where one hydroxyl groups rotates out of the 'c' conformation. The 'r' map differs considerably from the 'c' map, having a minimum at $\phi_H/\psi_H \sim -30°/-35°$ and no other low energy regions in the map area presented. The differences in the two maps are significant considering that the differences are in the hydroxyl groups directions. The hydration energy maps of these forms are similar; however the most negative hydration energy occurs near the energy minimum in the 'c' form but not near the minimum in the 'r' form.

gt′(r/c)–tg(r/c)

Figure 9a–d shows both 'r' and 'c' forms and hydration energies. Rather complex maps are found for both forms, with several local high energy minima. The 'c' map is fairly symmetric around the $\phi_H/\psi_H \sim 35°/-17°$ with a spread of dihedral values of ∼35° to the 1.0 kcal/mol contour. A second higher energy (∼3 kcal/mol) minimum occurs near $\phi_H/\psi_H \sim +30°/-80°$. In the 'r' map the second minimum occupies a much smaller space, but is lower in relative energy.

tg′(r/c)–tg(r/c)

In Fig. 10a–d is shown the map when both hydroxymethyl groups are in the tg conformation. The position of the minimum energy (see Fig. 10a) is close to 'r' forms previously presented, but shifted by ∼20° to smaller values in ϕ_H when compared to the 'c' forms. The ψ_H spread to the 1 kcal/mol isopotential contour is smaller than the allowable movement in the ϕ_H direction.

Figure 10c shows the maps for tg′(c)–tg(c) with the mixed basis set including COSMO. The energy minimum appears around $\phi_H/\psi_H \sim 30°/-25°$ with a

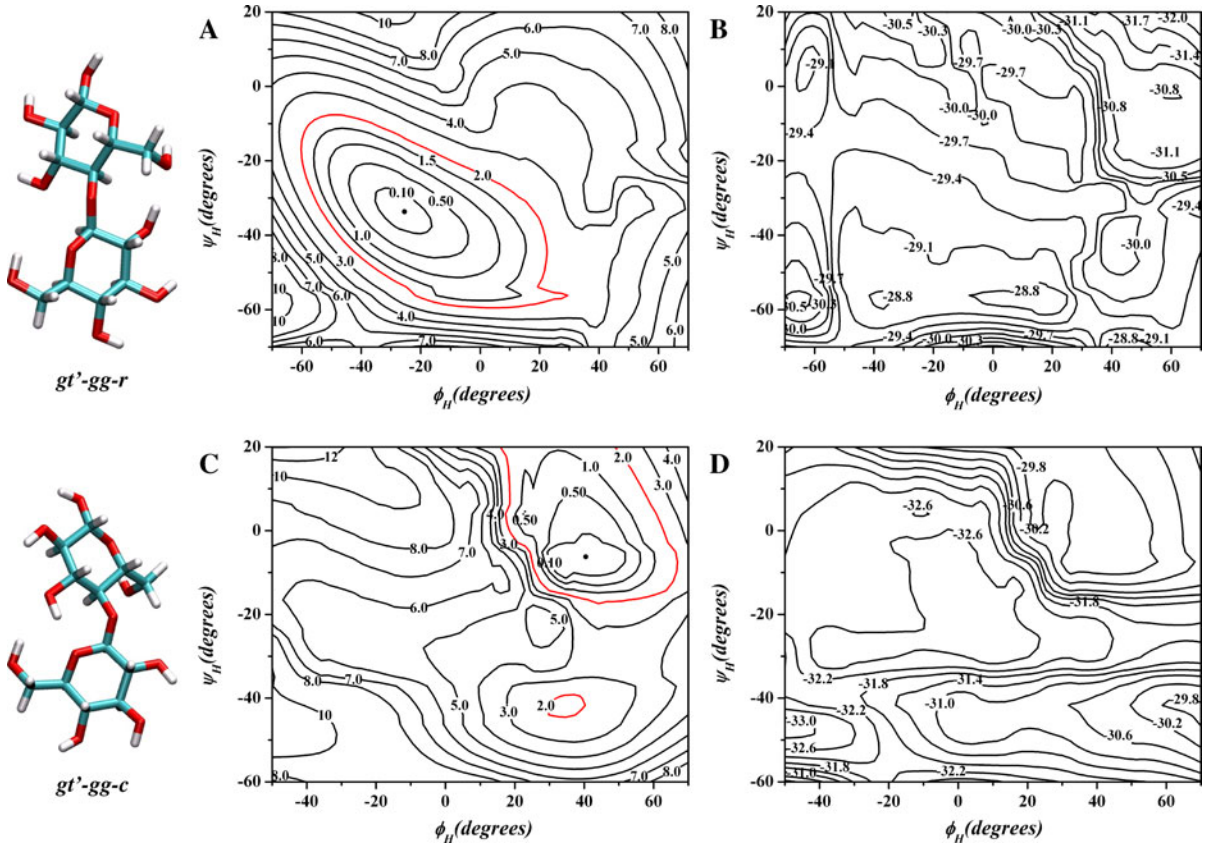

Fig. 7 Relaxed iso-potential (ϕ_H, ψ_H) maps for the gt′(c)′gt(c) conformations of β-cellobiose. The *contour lines* values are in kcal/mol and are relative to the lowest energy point. **a** E = −814,051.9 kcal/mol, DFTr in vacuo. **b** E = −814,480.0 kcal/mol, B3LYP/6-31+G*//DFTr in vacuo. **c** E = −814,511.0 kcal/mol, SolDFTr. **d** COSMO hydration energy at the B3LYP/6-31+G*//DFTr level of theory

slowly varying gradient giving a spread of ∼35° in ϕ_H and similarly in ψ_H to come to the 1.0 kcal/mol iso-potential contour. There are no interesting features in the map until regions of very high energy. The hydration energies are similar in the two maps.

tg′(r/c)–gg(r/c)

In Fig. 11a–d is shown two very different maps for the ‘r’ and ‘c’ forms of tg′–gg. The ‘r’ map has one energy minimum at ϕ_H/ψ_H ∼ −25°/−35°, while the ‘c’ map is of high energy at this position and has two low energy regions, the true minimum being at ϕ_H/ψ_H ∼ 30°/−10° and a second local minimum at ∼30°/−35°. The second position is not a true minimum for the all ‘c’ form since the ring 1 hydroxyl O2–H2 group has rotated to the ‘r’ direction. Hydration energies are not of lowest energy in the ‘r’ form, but are favorable around the lowest energy minimum in the ‘c’ form.

tg′(r/c)–gt(r/c)

Figure 12a–d shows the maps for both ‘r’ and ‘c’ forms of tg′–gt. Figure 12a shows two minima one at ∼40°/−20° and a second ∼1.0 kcal/mol higher in energy at ∼30°/−70°. It should be noted that the split in the map occurring around ψ_H ∼ −50° is caused by the rotation of the OH3′ from the ‘r’ orientation to a more ‘c’ like orientation to better interact with the O5 when ψ_H becomes less than −50°. (Formally, the reorientation could only be prevented by additionally constraining the torsion angle associated with the movement of OH3′ but this

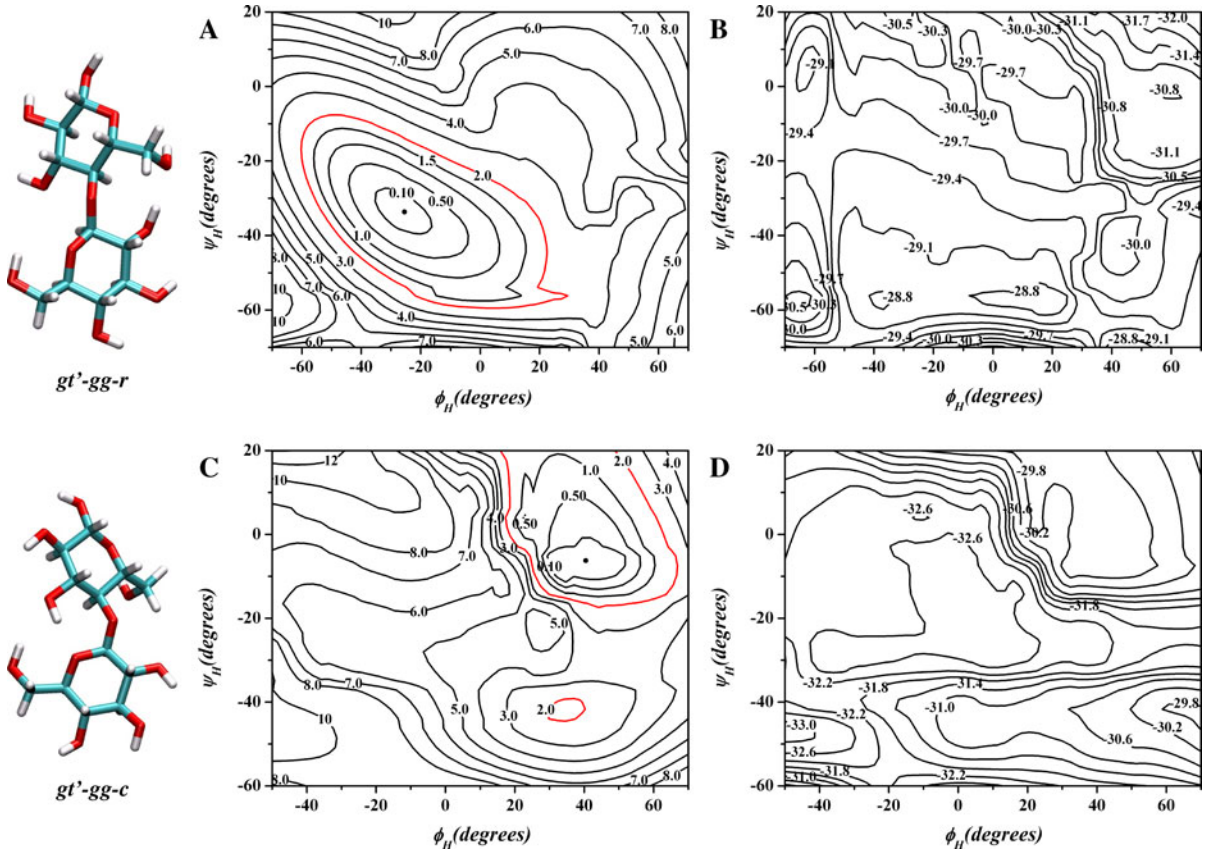

Fig. 8 Relaxed iso-potential (ϕ_H, ψ_H) maps for the gt′(r/c)–gg(r/c) conformations of β-cellobiose. The *contour lines* values are in kcal/mol and are relative to the lowest energy point. **a** gt′(r)–gg(r), E = −814,055.8 kcal/mol, DFTr in vacuo. **b** gt′(r)–gg(r), COSMO hydration energy at the B3LYP/6-31+G*//DFTr level of theory. **c** gt′(c)–gg(c), E = −814,053.8 kcal/mol, DFTr in vacuo. **d** gt′(c)–gg(c), COSMO hydration energy at the B3LYP/6-31+G*//DFTr level of theory

would skew the energetics of the map.) The reorientation of OH3 is surprisingly independent of the value of ϕ_H.

In the 'c' form of this combination of hydroxymethyl groups, the energy minimum appears around $\phi_H/\psi_H \sim 30°/-23°$ and the spread of low energy up to 1 kcal/mol is ∼30° in both dihedral angles. The 'c' form energy minimum is more normal, having only the one minimum energy position (see Fig. 12c).

Anti maps

Anti-forms are described in the next section. Characteristic for the *anti*-forms is that the value of ϕ_H or ψ_H is ∼180°.

gg′(r/c)–gg(r/c)–ϕ_H–*anti*

The maps (see Fig. 13a–f) of the ϕ_H–*anti*-forms show only slight differences in the contours between the vacuum and solvated states, with the 'r' maps having a somewhat sharp energy slope as ϕ_H becomes smaller than 170°. It is important to note that the gg′(r)–gg(r)–ϕ_H–*anti* is the lowest energy conformation found by optimization methods for in vacuo and the COSMO solvation optimization, as shown in Table 1. The 'c' form (ΔE ∼ 3.5 kcal/mol) is not improved in relative energy by COSMO solvation. In fact, the relative energy is larger than when in vacuo. Both the 'r' and the gg′(c)–gg(c)–ϕ_H–*anti* maps are very symmetric around ∼180°/0° with a spread in ϕ_H and ψ_H that, although smaller than the *syn* forms, is

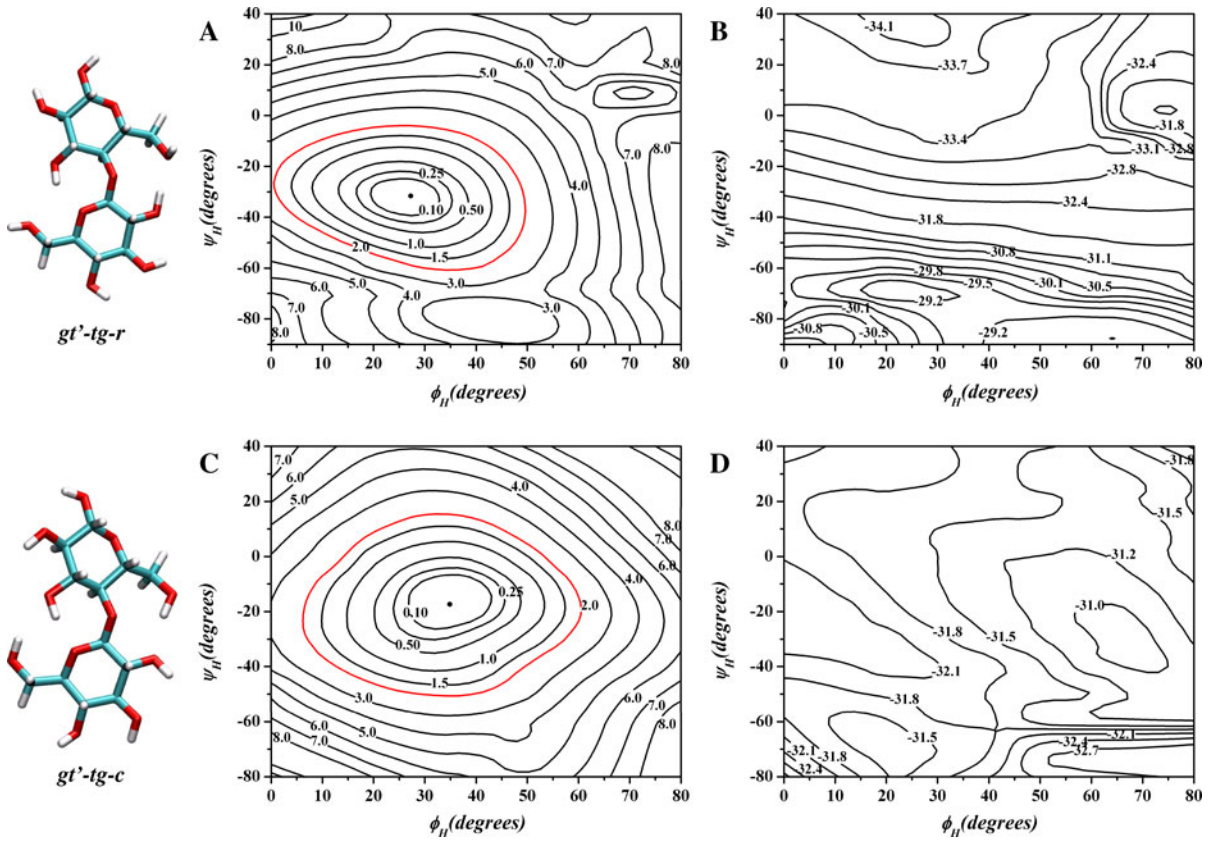

Fig. 9 Relaxed iso-potential (ϕ_H, ψ_H) maps for the gt′(r/c)–tg(r/c) conformations of β-cellobiose. The *contour lines* values are in kcal/mol and are relative to the lowest energy point. **a** gt′(r)–tg(r), E = −814,053.3 kcal/mol, DFTr in vacuo. **b** gt′(r)–tg(r), COSMO hydration energy at the B3LYP/6-31+G*//DFTr level of theory. **c** gt′(c)–tg(c), E = −814,052.2 kcal/mol, DFTr in vacuo. **d** gt′(c)–tg(c), COSMO hydration energy at the B3LYP/6-31+G*//DFTr level of theory

still fairly large, covering ∼25° in any direction to reach the 1.0 kcal/mol iso-potential contour. The energy minimum in both maps remains close to ϕ_H ∼ 170°–180°. The addition of COSMO does not influence the position of the energy minimum in either the 'r' or the 'c' case significantly. The average hydration energy for the 'r' form is ∼−27.4 kcal/mol, while the 'c' form average is ∼−26.4 kcal/mol, that is, hydration again favors 'r' as found for other conformations.

gg′(r/c)–gg(r/c)–ψ_H–*anti*

When ψ_H is rotated by ∼180° from the *syn* 'r' or 'c' form, the maps (Fig. 14a–f) have energy minima at ∼10°/185°. These maps are quite symmetric and have large low energy spreads of ∼35° in each direction to reach the 1.0 kcal/mol contour. The relative in vacuo energy of these forms is fairly high, ∼7–8 kcal/mol, but they are solvent favored having average hydration energies of ∼−30 kcal/mol, bringing the relative solvated energy down to ∼4 kcal/mol for the 'r' form. It is important to note that the 'r' form has a second minimum at ∼10°/185° approximately 1 kcal/mol higher in energy lying in a path pointing towards the gg′–gg–r *syn*-form (see Fig. 2a). This valley provides a direct pathway between the *anti* and *syn*-form with an approximate barrier of 2.5 kcal/mol in vacuo and ∼3.5 kcal/mol in solution.

gt′(r/c)–gt(r/c)–ϕ_H–*anti*

Figure 15a–f shows the nearly symmetric map for this form when the ϕ_H dihedral is rotated by ∼180°.

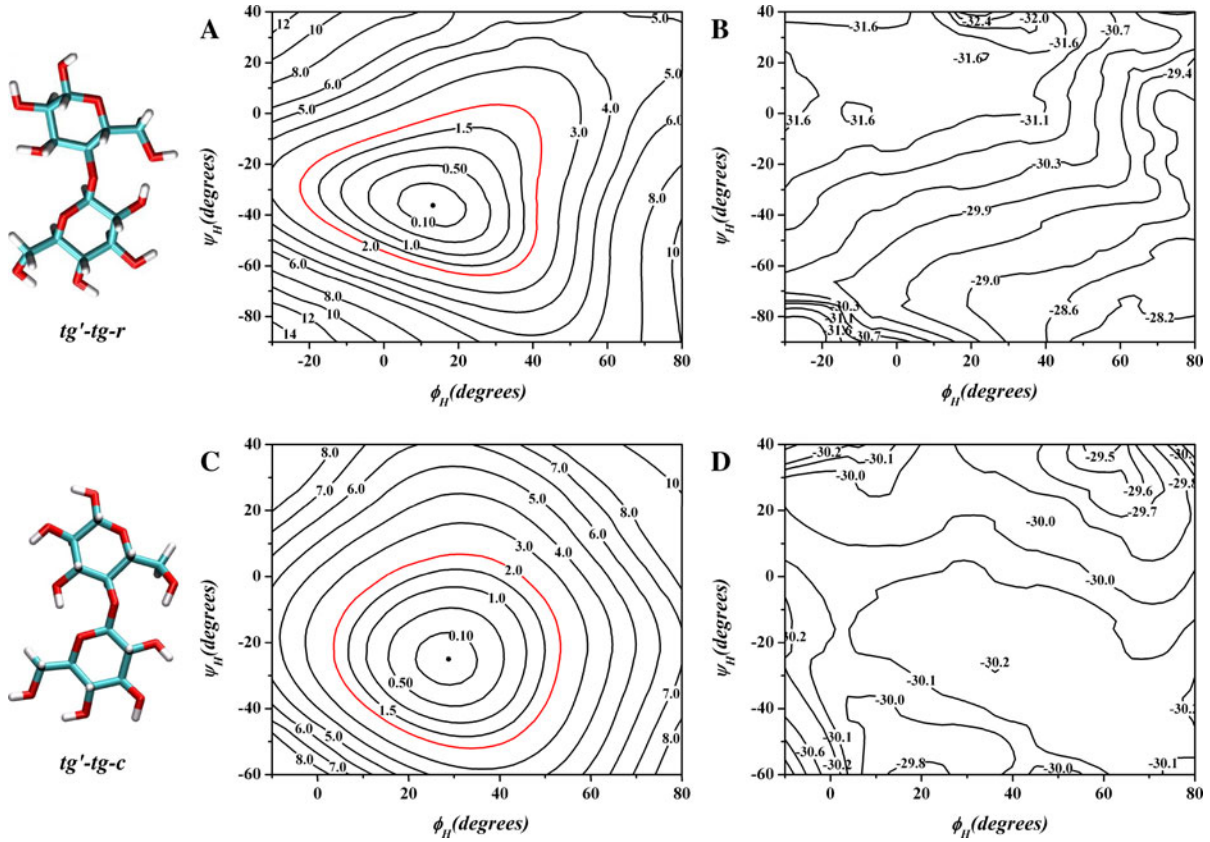

Fig. 10 Relaxed iso-potential (ϕ_H, ψ_H) maps for the tg′(r/c)–tg(r/c) conformations of β-cellobiose. The *contour lines* values are in kcal/mol and are relative to the lowest energy point. **a** tg′(r)–tg(r), E = −814,052.4 kcal/mol, DFTr in vacuo. **b** tg′(r)–tg(r), COSMO hydration energy at the B3LYP/6-31+G*//DFTr level of theory. **c** tg′(c)–tg(c), E = −814,054.7 kcal/mol, B3LYP DFTr in vacuo. **d** tg′(c)–tg(c), COSMO hydration energy at the B3LYP/6-31+G*//DFTr level of theory

The 'r' and 'c' maps for the *anti*-form are similar in shape with only slight movement in the position of minimum energy. There is of course a large difference in the absolute energy between these two *anti*-forms. The contour for 1.0 kcal/mol encloses a relatively small region of conformational space with a spread of ∼30° in ϕ_H and ψ_H. The relative energy of the hydrated 'r' form is low, being ∼2 kcal/mol relative to the in vacuo values of ∼3.5 kcal/mol, and this arises from the strong hydration energy of −29 kcal/mol at the minimum.

gt′(r/c)–gt(r/c)–ψ_H–*anti*

The maps, shown in Fig. 16a–f, show a rather large shift in the energy minimum, to a value in ϕ_H/ψ_H of ∼60°/210° for 'r' and ∼30°/170° for 'c', respectively. This is a significant shift for both the 'r' and 'c' forms, and is not observed so dramatically in the gg′–gg–ψ_H–*anti* forms. Note that to return to $\phi_H \sim 0°$ would take several kcal/mol in energy. The hydration does not change the relative energies significantly for the 'r' form, dropping the relative energy of the 'c' form by ∼2–3 to ∼5 kcal/mol. Similar to the gg′–gg–r–ψ_H–*anti* form there is a second minima in 'r' and again there is a valley connecting the *anti* with the *syn*-form (see Fig. 6a). The energy barrier between the *syn* and *anti* form is ∼3 kcal/mol for both the in vacuo and solvated structures. Looking ahead to the tg′–tg–r–ψ_H–*anti* form (see Fig. 18a–c) there is no double minima nor an obvious low energy pathway to the *syn*-form.

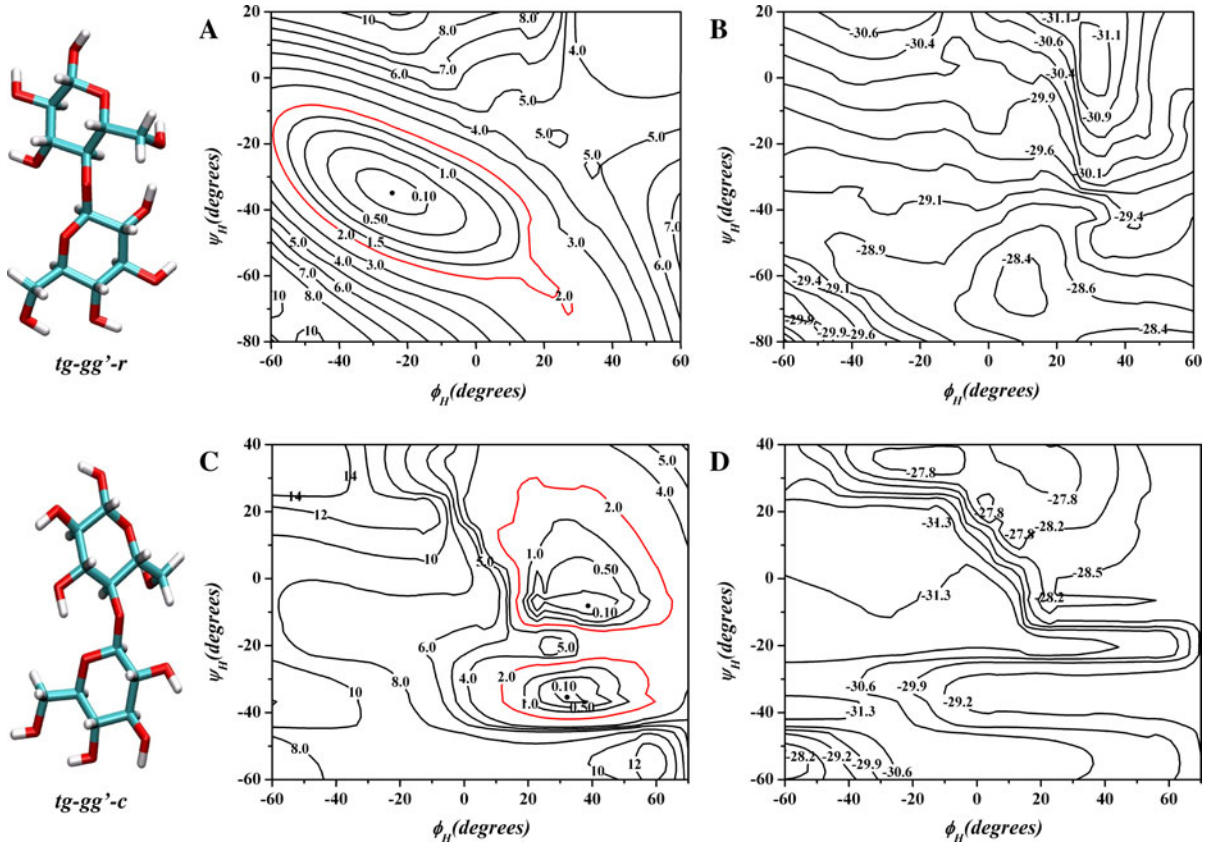

Fig. 11 Relaxed iso-potential (ϕ_H, ψ_H) maps for the tg′(r/c)–gg(r/c) conformations of β-cellobiose. The *contour lines* values are in kcal/mol and are relative to the lowest energy point. **a** tg′(r)–gg(r), E = −814,053.5 kcal/mol, DFTr in vacuo. **b** tg′(r)–gg(r), COSMO hydration energy at the B3LYP/6-31+G*//DFTr level of theory. **c** tg′(c)–gg(c), E = −814,054.9 kcal/mol, B3LYP DFTr in vacuo. **d** tg′(c)–gg(c), COSMO hydration energy at the B3LYP/6-31+G*//DFTr level of theory

tg′(r/c)–tg(r/c)–ϕ_H–*anti*

In Fig. 17a–f are shown the maps for the ϕ_H–*anti* forms of the ‘r’ and ‘c’ forms of tg′–tg–ϕ_H–*anti* conformers. The symmetric minimum energy positions are very close to the 180°/0° axis in both cases. The spread across in each direction to the 1.0 kcal/mol contour is ∼30°, again a fairly large low energy region for such a strained conformation.

The ‘c’ form of the tg′–tg–ϕ_H–*anti* conformer is shown in Fig. 17d. It would appear that it is of little difference in this case whether the hydroxyl groups are ‘r’ or ‘c’, the position of minimum energy remains symmetric and nearly the same position in each. The hydrated ‘r’ form is ∼2 kcal/mol in relative energy, having favorable hydration energy, but not one of the best hydration values. The ‘c’ relative energy is higher in energy than the ‘r’ form by ∼5 kcal/mol and has a more negative hydration energy (see Table 1).

tg′(r/c)–tg(r/c)–ψ_H–*anti*

These maps, shown in Fig. 18a–f, are very symmetric around ∼0°/180° in ϕ_H/ψ_H, and show a spread of low energy of ∼35° to reach the 1.0 kcal/mol contour. Again, this is a rather unexpected result, having rotated the C1′–O4–C4–H4 dihedral by 180°. The hydrated relative energies are both ∼6 kcal/mol with a range of hydration energy of −26 to −29 kcal/mol, for the ‘c’ and ‘r’ forms, respectively.

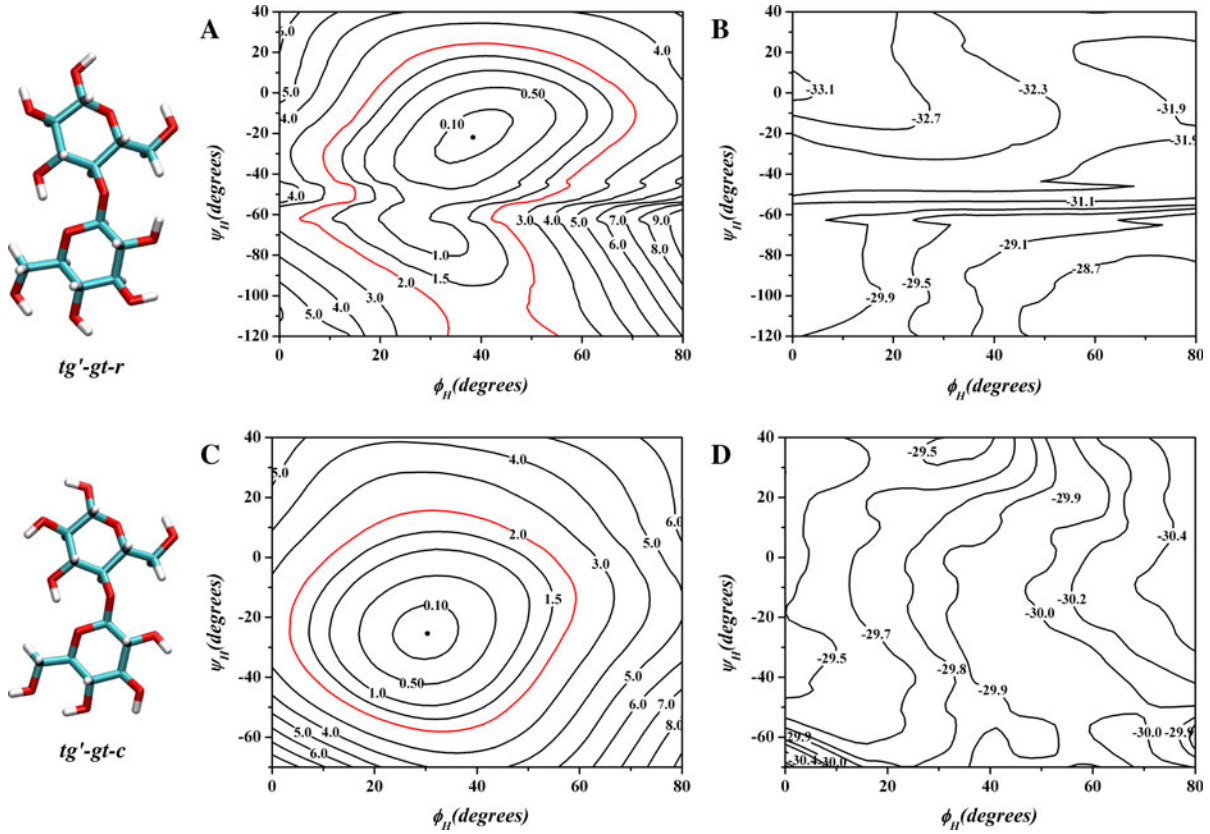

Fig. 12 Relaxed iso-potential (ϕ_H, ψ_H) maps for the tg′(r/c)–gt(r/c) conformations of β-cellobiose. The *contour lines* values are in kcal/mol and are relative to the lowest energy point. **a** tg′(r)–gt(r), E = −814,053.5 kcal/mol, DFTr in vacuo. **b** tg′(r)–gt(r), COSMO hydration energy at the B3LYP/6-31+G*//DFTr level of theory. **c** tg′(c)–gt(c), E = −814,054.0 kcal/mol, DFTr in vacuo. **d** tg′(c)–gt(c), COSMO hydration energy at the B3LYP/6-31+G*//DFTr level of theory

Anti–anti maps

In the next section is presented the results of both ϕ_H and ψ_H having a torsion angle of ∼180°, and the maps are denoted as *anti–anti* maps.

gg′(r/c)–gg(r/c)–*anti–anti*

In Fig. 19a–f the gg′(r/c)–gg(r/c)–*anti–anti* maps are presented. The positions of the energy minima differ going from the 'r' to the 'c' form. The gg′(r)–gg(r)–*anti–anti* form is not very stable compared to the other rotamer forms. The preferred form, which is the gg′(r)–gg(r)–ψ_H–*anti–anti* form, represents the overall minimum in Fig. 19a. The gg′(r)–gg(r)–*anti–anti* form has a very shallow minimum at ∼179°/215° with a relative energy of ∼12 kcal/mol greater than the gg′(r)–gg(r)–ψ_H–*anti–anti* minimum.

Figure 19d shows the map for the 'c' form, the position of minimum energy is ∼186°/201° and symmetric around the minimum showing a spread of low energy space of ∼30° in both ϕ_H and ψ_H. The relative energy for the *anti–anti* forms is high, being in the 12–13 kcal/mol range when solvated, 15–16 kcal/mol when in vacuo. The average hydration energy is in the −29 to −30 kcal/mol range.

gt′(r/c)–gt(r/c)–*anti–anti*

The *anti–anti* maps are shown in Fig. 20a–f. Clearly, the 'r' map is tightly held at the minimum energy position and small variation in ψ_H quickly brings an increase in energy in either direction. The spread to the 1.0 kcal/mol contour is very *anti*-symmetric, elongating from ∼170° toward larger ϕ_H values

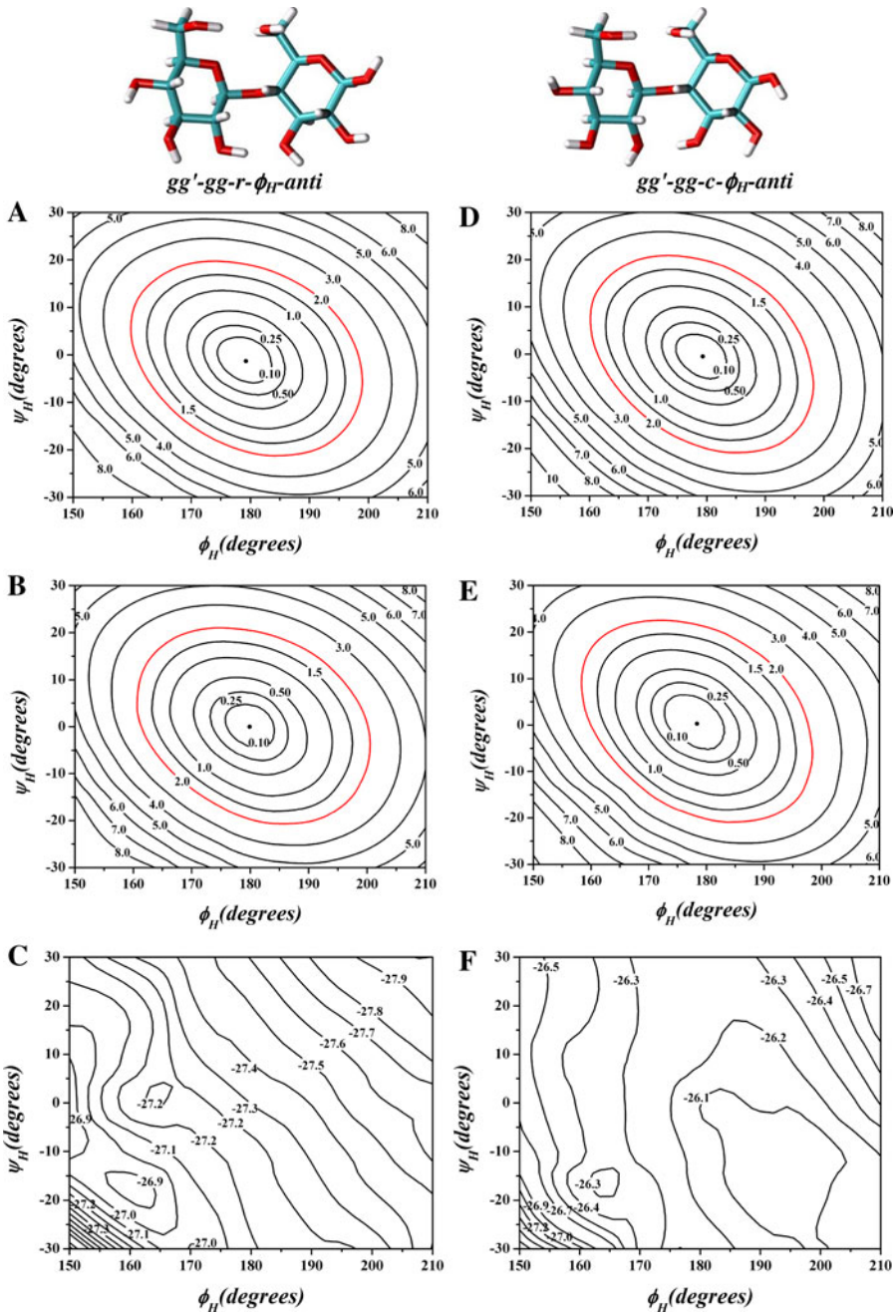

Fig. 13 Relaxed iso-potential (ϕ_H, ψ_H) maps for the gg′(r/c)–gg(r/c)-ϕ_H–*anti* conformations of β-cellobiose. The *contour lines* values are in kcal/mol and are relative to the lowest energy point. **a** gg′(r)–gg(r)-ϕ_H–*anti*, E = −814,060.0 kcal/mol, DFTr in vacuo. **b** gg′(c)–gg(c)-ϕ_H–*anti*, E = −814,515.0 kcal/mol, SolDFTr. **c** gg′(r)–gg(r)-ϕ_H–*anti*, COSMO hydration energy at the B3LYP/6-31+G*//DFTr level of theory. **d** gg′(c)–gg(c)-ϕ_H–*anti*, E = −814,057.6 kcal/mol, DFTr in vacuo. **e** gg′(c)–gg(c)-ϕ_H–*anti*, E = −814,511.5 kcal/mol, SolDFTr. **f** gg′(c)–gg(c)-ϕ_H–*anti*, COSMO hydration energy at the B3LYP/6-31+G*//DFTr level of theory

while remaining of low relative energy (relative to the position of minimum energy).

The positions of minimum energy for the 'c' form are shifted somewhat away from the 180° position, being ∼189° and 200° in ϕ_H and ψ_H, but having fairly large spreads ∼30° in dihedral angles to reach the iso-potential contour of 1.0 kcal/mol in energy. In other words, although this region of conformational space is of high energy, the flexibility is only slightly impaired relative to that of the *syn* forms. The relative energy of this set of conformers is in the range of 11 kcal/mol while the hydration energy of the 'r' form is the most negative value of all the conformations (−32.8 kcal/mol), lowering the relative energy from ∼16 kcal/mol in vacuo to 10.7 kcal/mol when hydrated.

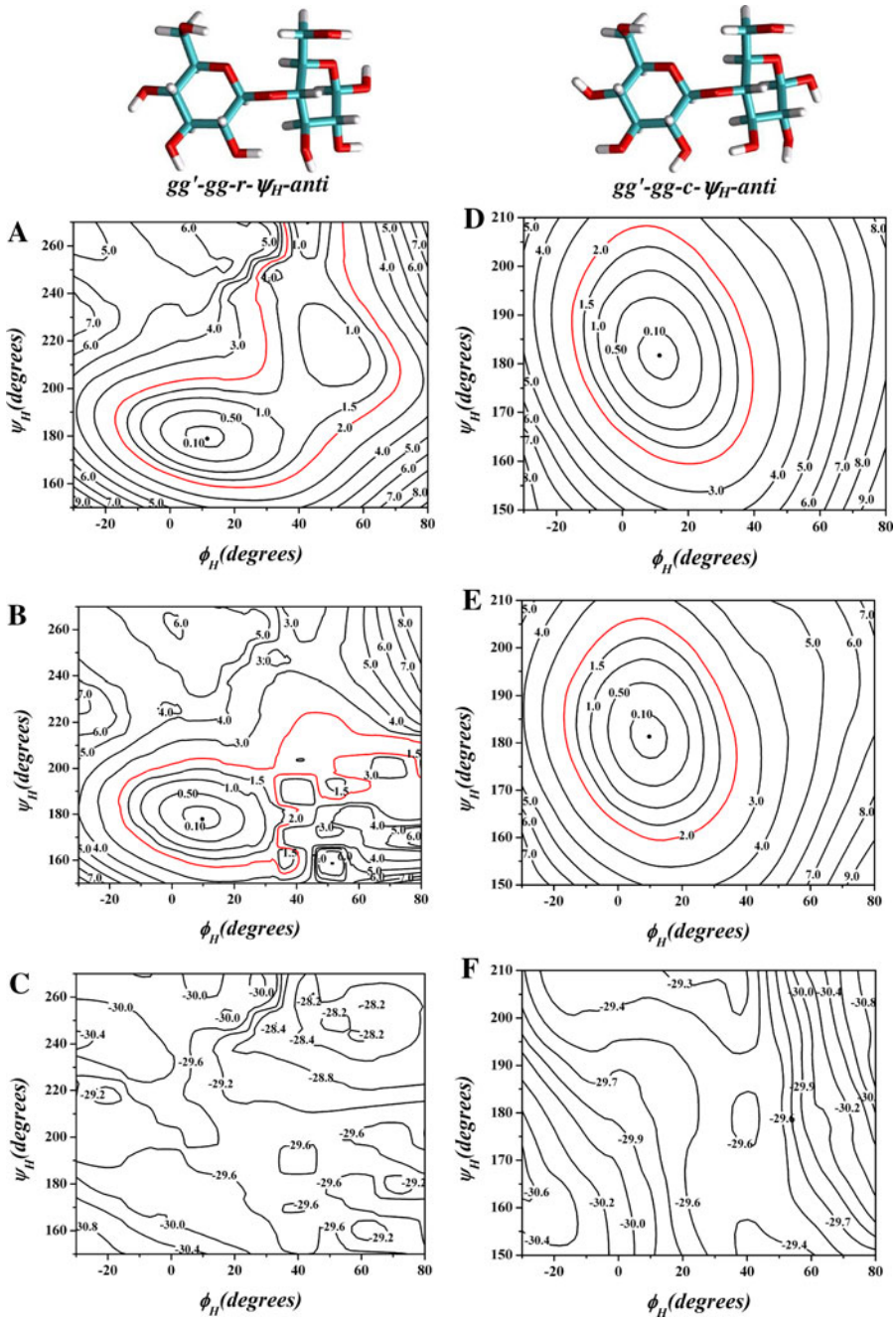

Fig. 14 Relaxed isopotential (ϕ_H, ψ_H) maps for the gg′(r/c)–gg(r/c)–ψ_H–*anti* conformations of β-cellobiose. The *contour lines* values are in kcal/mol and are relative to the lowest energy point. **a** gg′(r)–gg(r)–ψ_H–*anti*, E = −814,053.1 kcal/mol, DFTr in vacuo. **b** gg′(c)–gg(c)–ψ_H–*anti*, E = −814,510.9 kcal/mol, SolDFTr. **c** gg′(r)–gg(r)–ψ_H–*anti*, COSMO hydration energy at the B3LYP/6-31+G*//DFTr level of theory. **d** gg′(c)–gg(c)–ψ_H–*anti*, E = −814,051.3 kcal/mol, DFTr in vacuo. **e** gg′(c)–gg(c)–ψ_H–*anti*, E = −814,509.3 kcal/mol, SolDFTr. **f** gg′(c)′gg(c)–ψ_H–*anti*, COSMO hydration energy at the B3LYP/6-31+G*//DFTr level of theory

tg′(r/c)–tg(r/c)–*anti*–*anti*

One may expect that the *anti*–*anti* form with both residues in the tg hydroxymethyl position would be rather difficult to move at the glycosidic bonds. However, again this preconceived notion is mistaken (see Fig. 21a–f), with the spread of dihedral angles around the lowest energy region being somewhat larger than the spread found for the *syn* forms. The ‘r’ form has a minimum at ∼178°/198° with a spread of low energies somewhat larger in the ϕ_H direction than in the ψ_H direction. Of interest in the ‘c’ form is the appearance of two minima in the regions of ∼187°/197° and ∼170°/220° in ϕ_H and ψ_H. The first

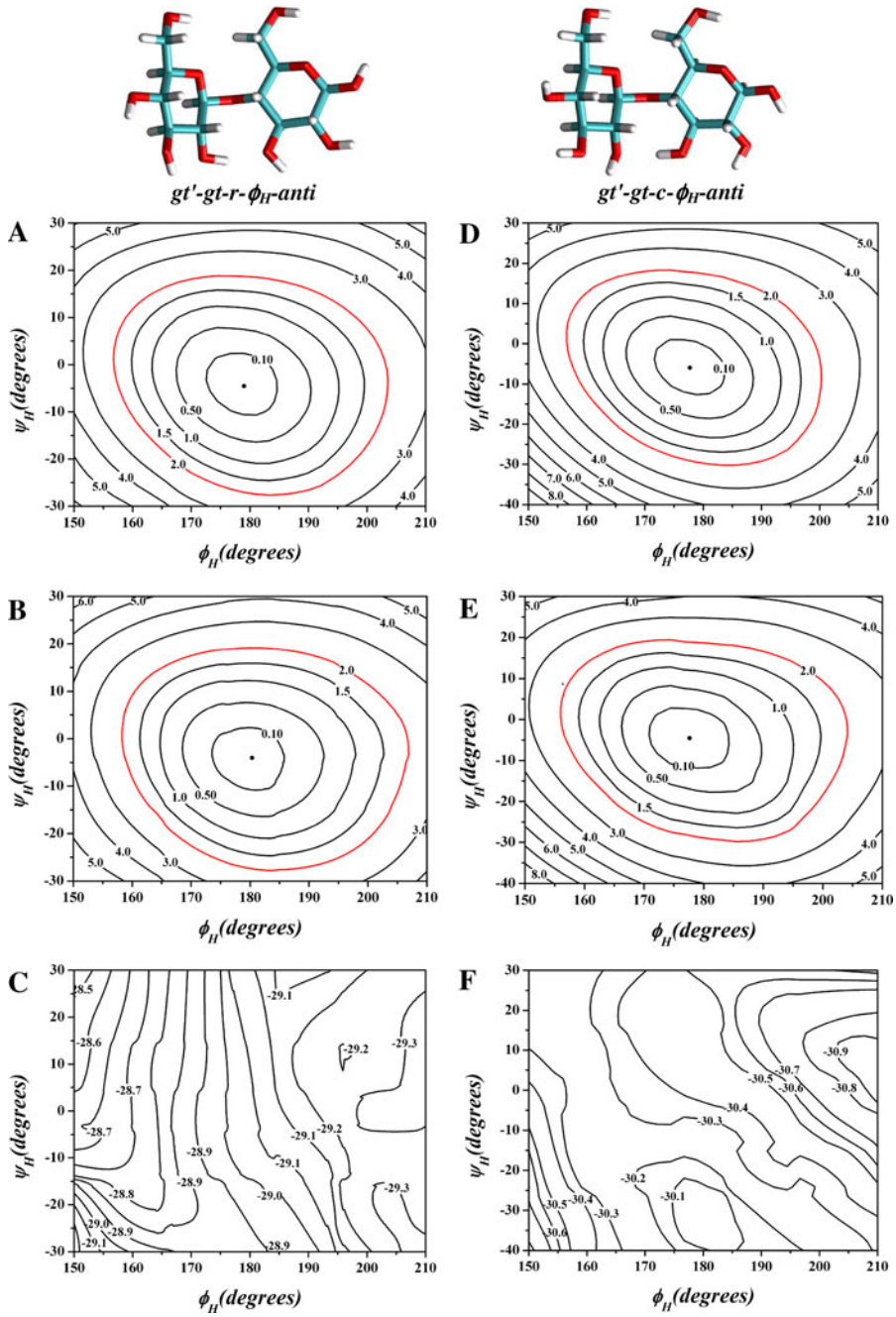

Fig. 15 Relaxed isopotential (ϕ_H, ψ_H) maps for the gt′(r/c)–gt(r/c)–ϕ_H–*anti* conformations of β-cellobiose. The *contour lines* values are in kcal/mol and are relative to the lowest energy point. **a** gt′(r)–gt(r)–ϕ_H–*anti*, E = −814,056.7 kcal/mol, DFTr in vacuo. **b** gt′(r)–gt(r)–ϕ_H–*anti*, E = −814,513.1 kcal/mol, SolDFTr. **c** gt′(r)–gt(r)–ϕ_H–*anti*, COSMO hydration energy at the B3LYP/6-31+G*//DFTr level of theory. **d** gt′(c)–gt(c)–ϕ_H–*anti*, E = −814,051.4 kcal/mol, DFTr in vacuo. **e** gt′(c)–gt(c)–ϕ_H–*anti*, E = −814,509.6 kcal/mol, SolDFTr. **f** gt′(c)–gt(c)–ϕ_H–*anti*, COSMO hydration energy at the B3LYP/6-31+G*//DFTr level of theory

minimum is ∼3.0 kcal/mol higher in energy than the lowest energy form and arises from a conformational transition to the tg′–gg forms during the optimization. However, the second minimum is of equal energy to the lowest energy form, and is a transition of the H6–O6 hydroxyl on the reducing residue moving from the gauch− to a gauch+ conformation. As the ϕ_H and ψ_H variation takes place this hydroxymethyl group is impacted sufficiently to rotate the H6–O6 group, expanding the allowable region of motion considerably. Remembering of course that these are high energy forms, and will most likely be of very low population, it is probable that the additional energy from increase entropy will not be significant. The

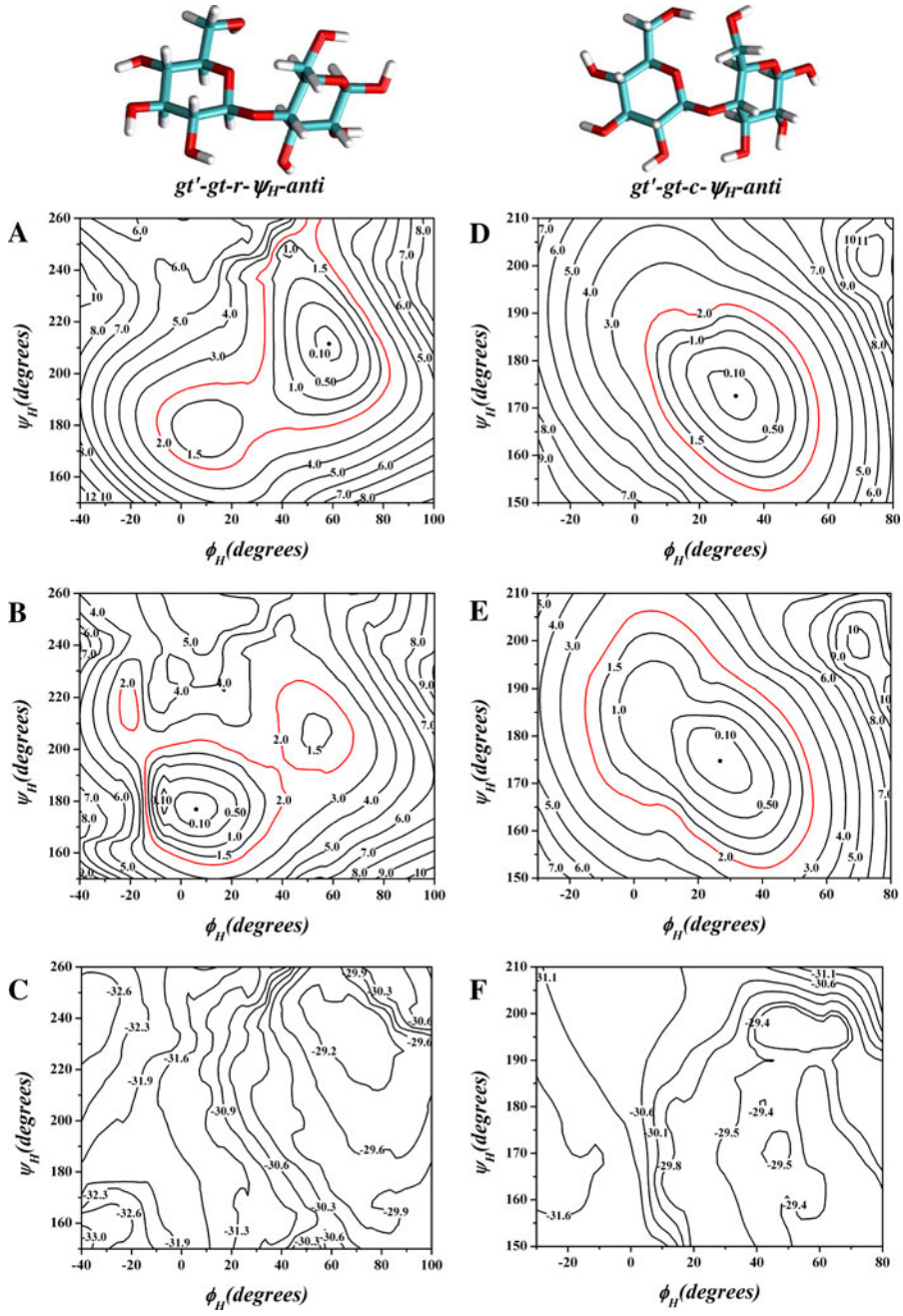

Fig. 16 Relaxed isopotential (ϕ_H, ψ_H) maps for the gt′(r/c)–gt(r/c)–ψ_H–*anti* conformations of β-cellobiose. The *contour lines* values are in kcal/mol and are relative to the lowest energy point. **a** gt′(r)–gt(r)–ψ_H–*anti*, E = −814,050.2 kcal/mol, DFTr in vacuo. **b** gt′(r)–gt(r)–ψ_H–*anti*, E = −814,510.5 kcal/mol, SolDFTr. **c** gt′(r)–gt(r)–ψ_H–*anti*, COSMO hydration energy at the B3LYP/6-31+G*//DFTr level of theory. **d** gt′(c)–gt(c)–ψ_H–*anti*, E = −814,052.2 kcal/mol, B3LYP and mixed basis set in vacuo. **e** gt′(c)–gt(c)–ψ_H–*anti*, E = −814,509.8 kcal/mol, SolDFTr. **f** gt′(c)–gt(c)–ψ_H–*anti*, COSMO hydration energy at the B3LYP/6-31+G*//DFTr level of theory

relative hydrated energies lie in the 12–13 kcal/mol range, with hydration energy range of ∼−29 to −30 kcal/mol.

Composite (“adiabatic”) maps

In Fig. 22 are shown in vacuo (A) and COSMO (B) composite maps, in which each conformation can (depending on the relative energy), contribute to a point on the map. A “true” adiabatic map for cellobiose would be computationally impractical to obtain in the context of this work, since all possible combinations of the secondary hydroxyls and hydroxymethyl groups would be necessary. However, this map shows clearly that in the *syn* region of conformational space, there are two unique minima,

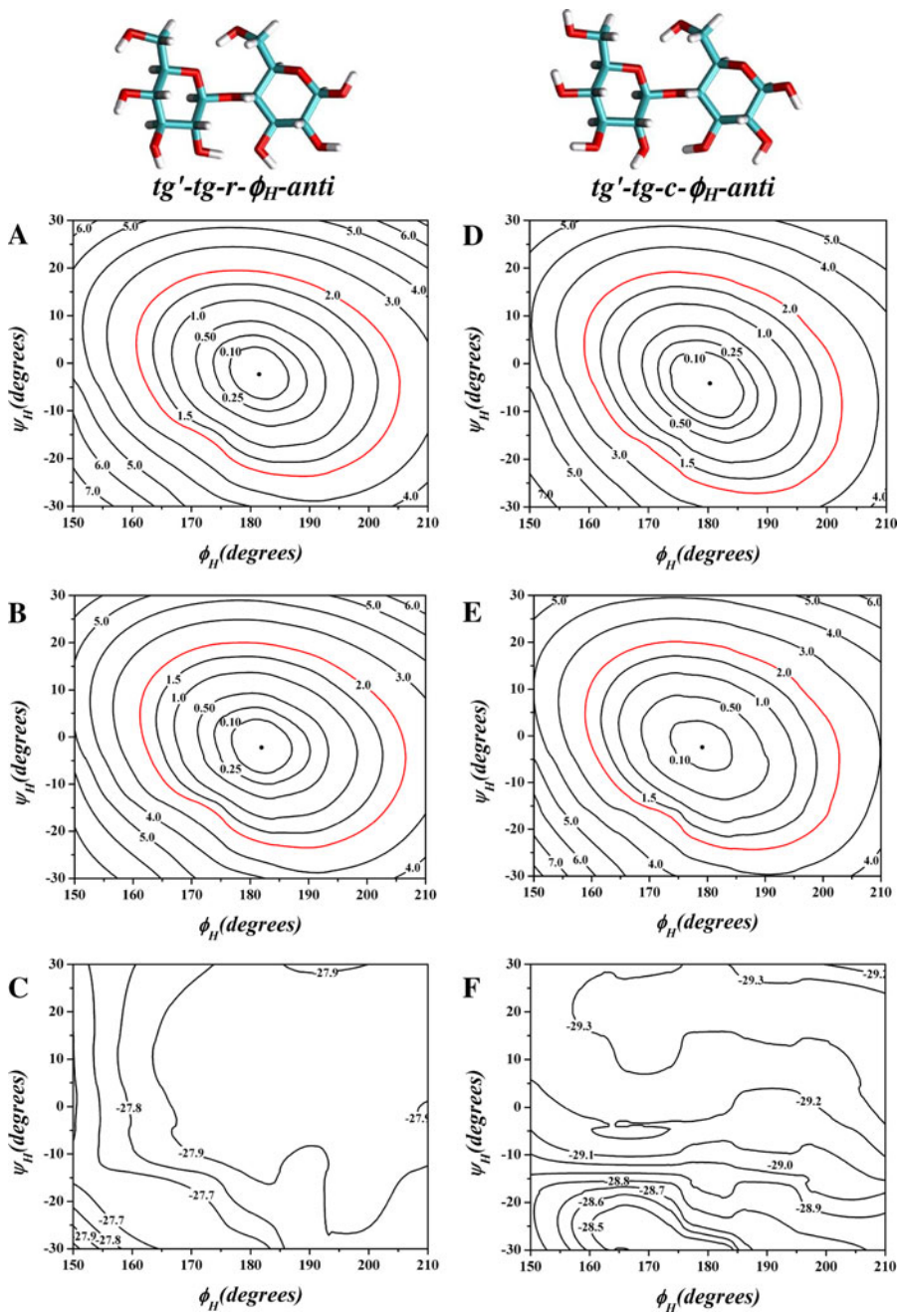

Fig. 17 Relaxed isopotential (ϕ_H, ψ_H) maps for the tg′(r/c)–tg(r/c)–ϕ_H–*anti* conformations of β-cellobiose. The *contour lines* values are in kcal/mol and are relative to the lowest energy point. **a** tg′(r)–tg(r)–ϕ_H–*anti*, E = −814,057.6 kcal/mol, DFTr in vacuo. **b** tg′(r)–tg(r)–ϕ_H–*anti*, E = −814,513.0 kcal/mol, SolDFTr. **c** tg′(r)–tg(r)–ϕ_H–*anti*, COSMO hydration energy at the B3LYP/6-31+G*//DFTr level of theory. **d** tg′(c)–tg(c)–ϕ_H–*anti*, E = −814,052.9 kcal/mol, DFTr in vacuo. **e** tg′(c)–tg(c)–ϕ_H–*anti*, E = −814,509.7 kcal/mol, SolDFTr. **f** tg′(c)–tg(c)–ϕ_H–*anti*, COSMO hydration energy at the B3LYP/6-31+G*//DFTr level of theory

the lowest energy in vacuo minimum changing from the region $\phi_H/\psi_H \sim -30°/-40°$, to $\phi_H/\psi_H \sim 35°/-30°$ upon addition of solvent. This is a major shift in lowest energy position. That is, the region of higher in vacuo energy in the *syn* region becomes the favored state upon addition of solvent. It should be noted that the ϕ_H–*anti* or flipped conformation remains lower in enthalpic energy than any of the *syn* forms, which require entropy contributions to be favored by free energy. This is suggested in the larger low energy region around the *syn* forms. Composite maps have been produced previously using empirical computational methods (French 1988; Vietor et al. 2000; French and Johnson 2004, 2009; Mendonca

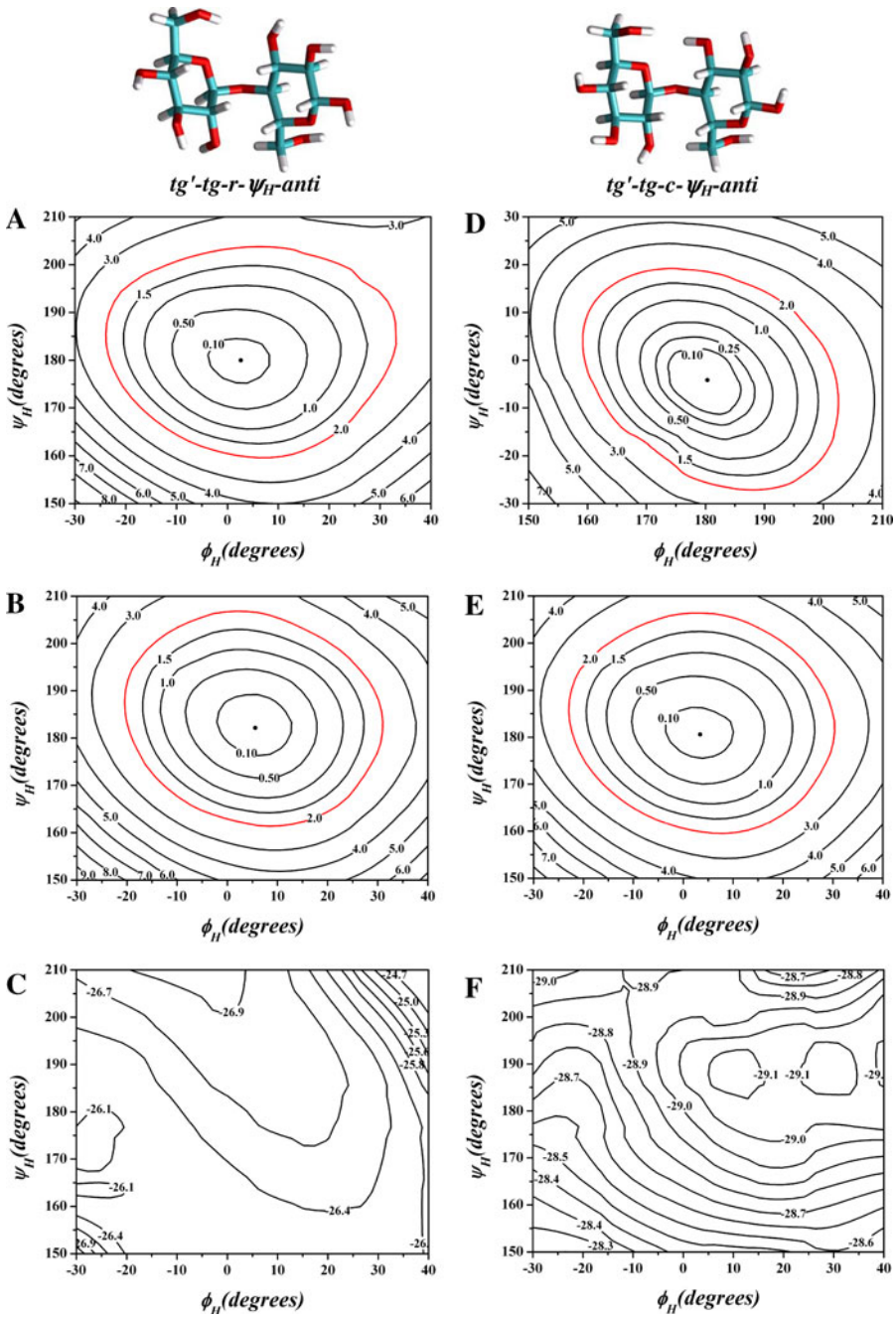

Fig. 18 Relaxed isopotential (ϕ_H, ψ_H) maps for the tg′(r/c)–tg(r/c)–ψ_H–*anti* conformations of β-cellobiose. The *contour lines* values are in kcal/mol and are relative to the lowest energy point. **a** tg′(r)–tg(r)-ψ_H–*anti*, E = −814,054.1 kcal/mol, DFTr in vacuo. **b** tg′(r)–tg(r)–ψ_H–*anti*, E = −814,508.6 kcal/mol, SolDFTr. **c** tg′(r)–tg(r)–ψ_H–*anti*, COSMO hydration energy at the B3LYP/6-31+G*//DFTr level of theory. **d** tg′(c)–tg(c)–ψ_H–*anti*, E = −814,051.7 kcal/mol, DFTr in vacuo. **e** tg′(c)–tg(c)–ψ_H–*anti*, E = −814,508.644 kcal/mol, SolDFTr. **f** tg′(c)–tg(c)–ψ_H–*anti*, COSMO hydration energy at the B3LYP/6-31+G*//DFTr level of theory

et al. 2002; Stortz and Cerezo 2003; Christensen et al. 2010). As a matter of content, most adiabatic maps convey sparse detail of the structures at each minimum and those maps are of little value to those wishing to understand the relative energies of these complex carbohydrates.

Energy relationships

The energy values in Table 1 give interesting information as to the solvent preferred conformations. Clearly, both the *syn* and *anti*-conformations appear to benefit from addition of solvent more than the *syn* conformers.

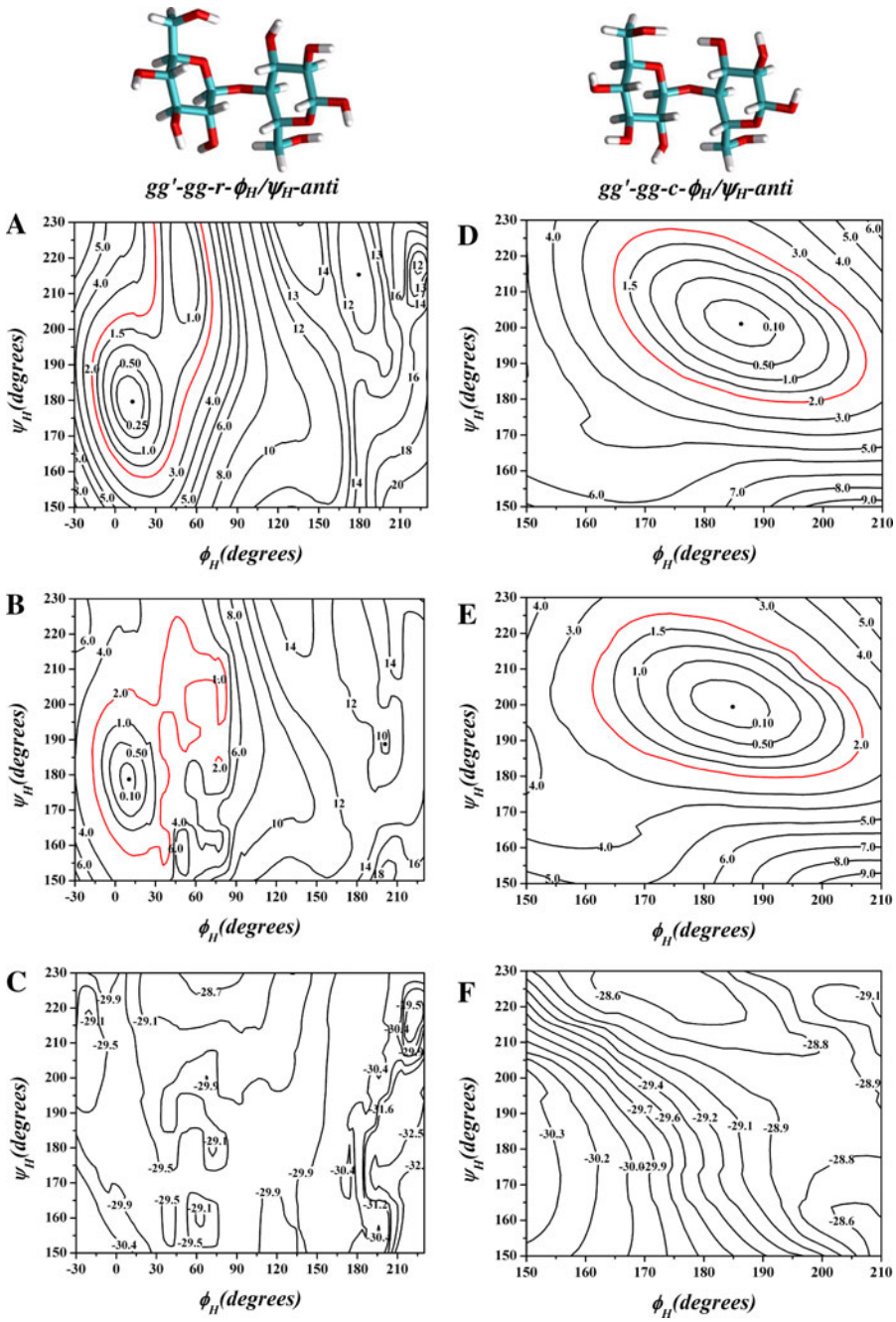

Fig. 19 Relaxed isopotential (ϕ_H, ψ_H) maps for the gg′(r/c)–gg(r/c)–ϕ_H/ψ_H–*anti–anti* conformations of β-cellobiose. The *contour lines* values are in kcal/mol and are relative to the lowest energy point. **a** gg′(r)–gg(r)–ϕ_H/ψ_H–*anti–anti*, E = −814,043.6 kcal/mol, DFTr in vacuo. **b** gg′(r)–gg(r)–ϕ_H/ψ_H–*anti–anti*, E = −814,501.5 kcal/mol, SolDFTr. **c** gg′(r)–gg(r)–ϕ_H/ψ_H–*anti–anti*, COSMO hydration energy at the B3LYP/6-31+G*// DFTr level of theory. **d** gg′(c)–gg(c)–ϕ_H/ψ_H–*anti–anti*, E = −814,046.0 kcal/mol, DFTr in vacuo. **e** gg′(c)–gg(c)–ϕ_H/ψ_H–*anti–anti*, E = −814,502.9 kcal/mol, SolDFTr. **f** gg′(c)–gg(c)–ϕ_H/ψ_H–*anti–anti*, COSMO hydration energy at the B3LYP/6-31+G*// DFTr level of theory

Most importantly, the relative energy differences between the in vacuo data and the solvated data are very significant. The order of conformations, as a result of the energy differences, change with application of solvent with relative energy differences of from ∼2 to 5 kcal/mol, suggesting that population analysis without solvent effects included could be significantly in error.

Conclusion

The use of an implicit solvent model within the DFT computational method has considerable impact on the solution structures of β-cellobiose, changing relative energies dramatically, moving positions of minimum energy by over 40°–50° in dihedral angles, and

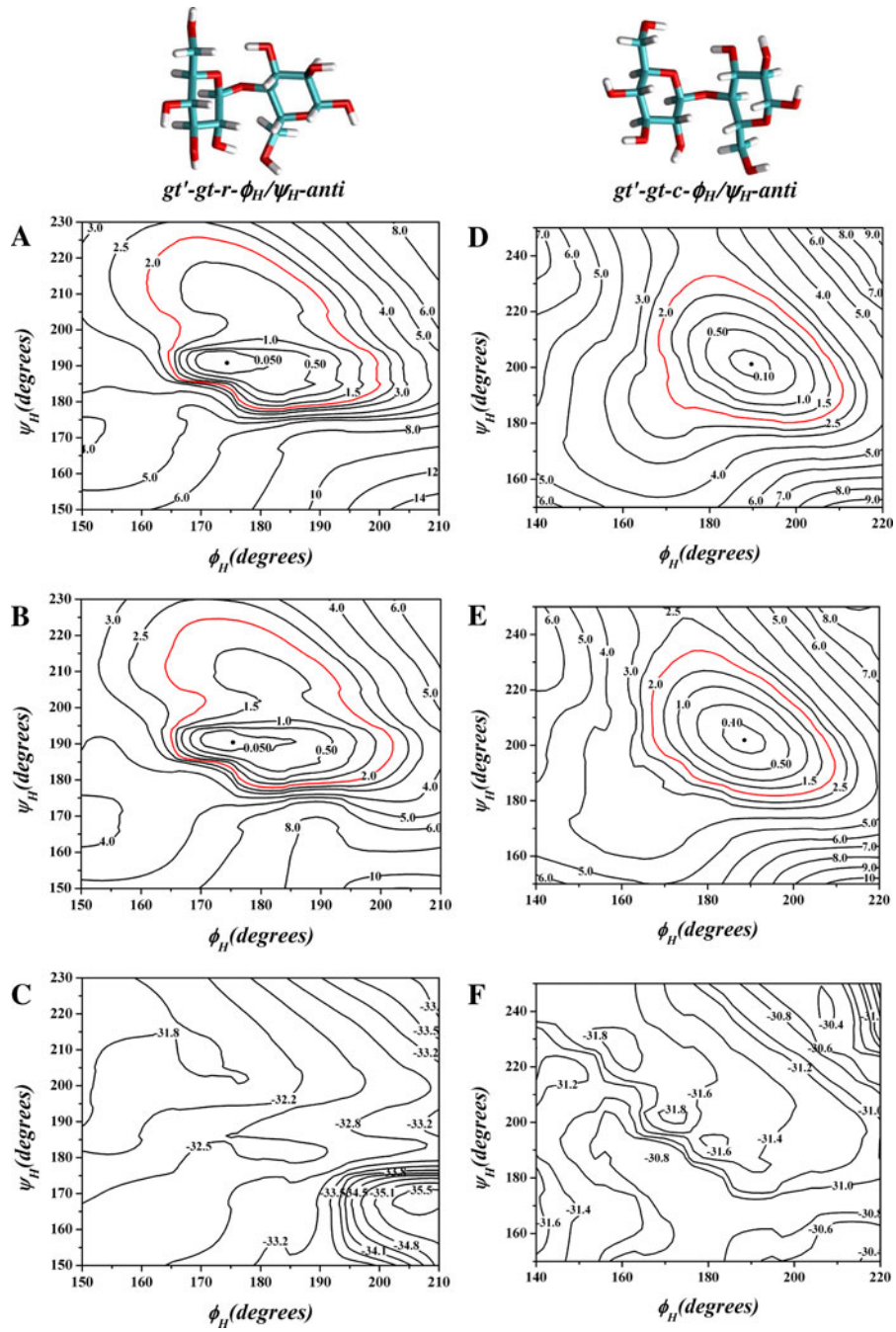

Fig. 20 Relaxed isopotential (ϕ_H, ψ_H) maps for the gt′(r/c)–gt(r/c)–ϕ_H/ψ_H–*anti–anti* conformations of *β*-cellobiose. The *contour lines* values are in kcal/mol and are relative to the lowest energy point. **a** gt′(r)–gt(r)–ϕ_H/ψ_H–*anti–anti*, E = −814,043.9 kcal/mol, DFTr in vacuo. **b** gt′(r)–gt(r)–ϕ_H/ψ_H–*anti–anti*, E = −814,504.3 kcal/mol, SolDFTr. **c** gt′(r)–gt(r)–ϕ_H/ψ_H–*anti–anti*, COSMO hydration energy at the B3LYP/6-31+G*// DFTr level of theory. **d** gt′(c)–gt(c)–ϕ_H/ψ_H–*anti–anti*, E = −814,043.9 kcal/mol, DFTr in vacuo.**e** gt′(c)–gt(c)–ϕ_H/ψ_H–*anti–anti*, E = −814,503.6 kcal/mol, SolDFTr. **f** gt′(c)–gt(c)–ϕ_H/ψ_H–*anti–anti*, COSMO hydration energy at the B3LYP/6-31+G*//DFTr level of theory

suggesting that ‘r’ solvated forms are of higher probability than the ‘c’ solvated forms. This result is in some conflict with other studies (da Silva and Nascimento 2004) in which they find that their maps obtained in aqueous solution shows regions of minimum energy in the same positions of the regions found in the map calculated in the gas phase. Although this is true in some cases, showing all of the maps individually allows one to digest which combinations of conformational parameters will be of low energy, and in which regions of ϕ_H/ψ_H space they will dominate the population.

A comparison of crystallographic and NMR data (Ham and Williams 1970; Leung et al. 1976; Duus et al.

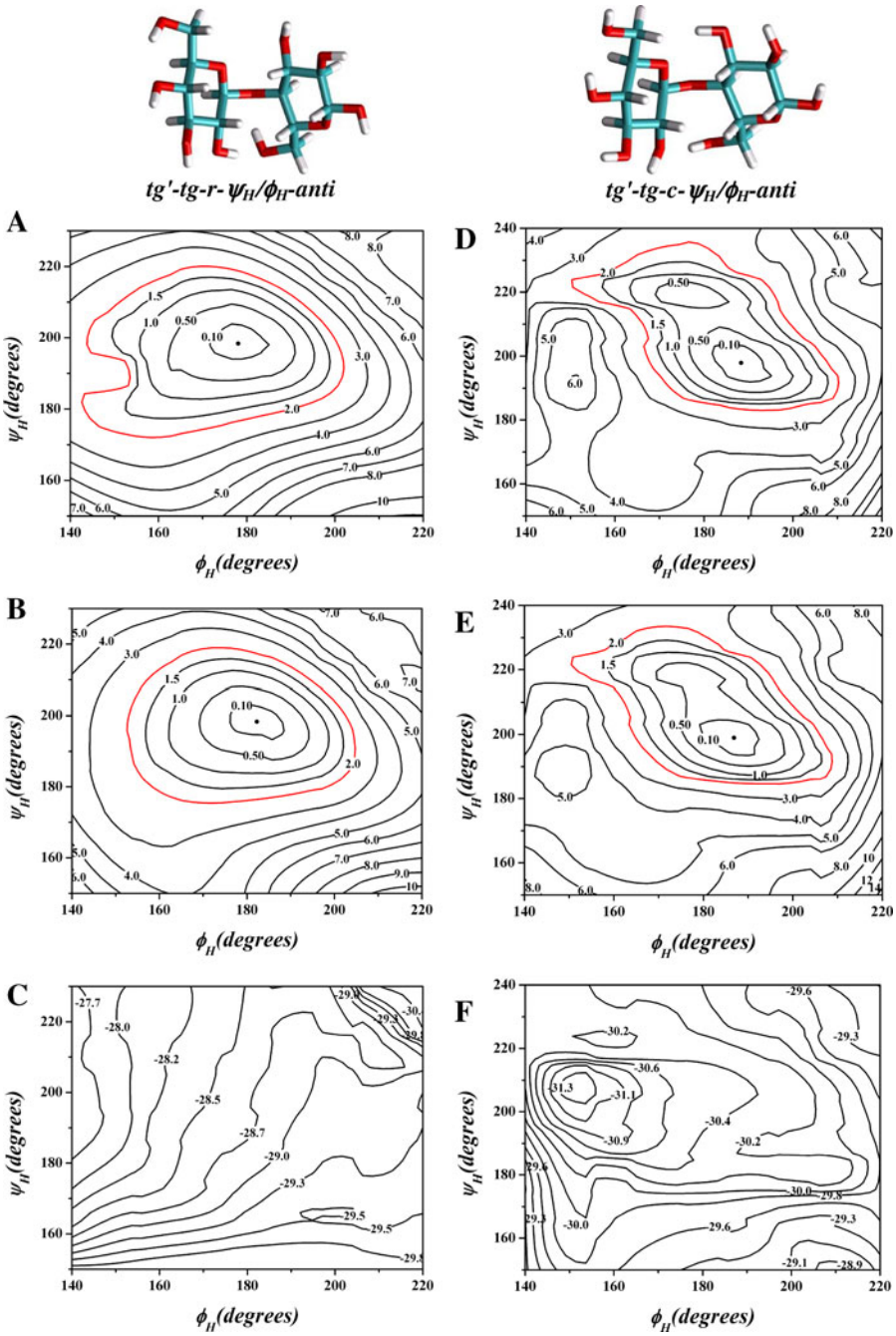

Fig. 21 Relaxed isopotential (ϕ_H, ψ_H) maps the tg′(r/c)–tg(r/c)–ϕ_H/ψ_H–*anti–anti* conformations of β-cellobiose. The *contour lines* values are in kcal/mol and are relative to the lowest energy point. **a** tg′(r)–tg(r)–ϕ_H/ψ_H–*anti–anti*, E = −814,045.7 kcal/mol, DFTr in vacuo. **b** tg′(r)-tg(r)–ϕ_H/ψ_H–*anti–anti*, E = −814,502.3 kcal/mol, SolDFTr. **c** tg′(r)–tg(r)–ϕ_H/ψ_H–*anti–anti*, COSMO hydration energy at the B3LYP/6-31+G*// DFTr level of theory. **d** tg′(c)–tg(c)–ϕ_H/ψ_H–*anti–anti*, E = −814,043.8 kcal/mol, DFTr in vacuo. **e** tg′(c)–tg(c)–ϕ_H/ψ_H–*anti–anti,* E = −814,502.4 kcal/mol, SolDFTr. **f** tg′(c)–tg(c)-ϕ_H/ψ_H–*anti–anti*, COSMO hydration energy at the B3LYP/6-31+G*// DFTr level of theory

1994; Hardy et al. 1996; Sugiyama et al. 2000; Wacowich-Sgarbi et al. 2001; Rencurosi et al. 2002; Cheetham et al. 2003; Larsson et al. 2004; Sergeyev and Moyna 2005; Yoneda et al. 2008; Olsson et al. 2008; Cocinero et al. 2009; Shen et al. 2009; Zhang et al. 2009) can be made with the results presented here. The experimental studies show that the ϕ_H and ψ_H dihedral angle positions shift for different hydroxymethyl conformation and hydroxyl orientations. For example, methyl β-cellobioside (Ham and Williams 1970) with the hydroxymethyl gt′–gg conformation, has ϕ_H/ψ_H values of 32°/−44°, while methyl β-cellotrioside

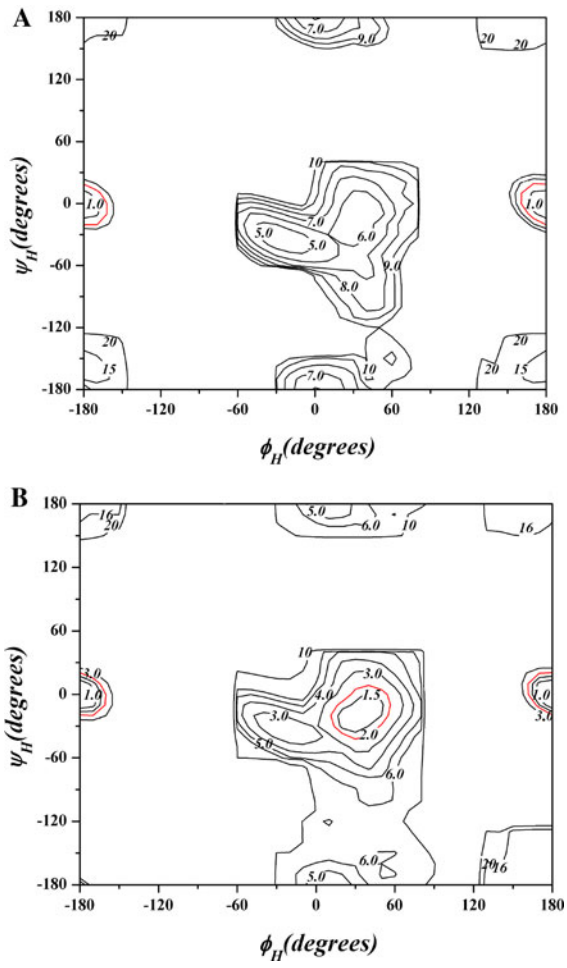

Fig. 22 Composite relaxed iso-potential (ϕ_H, ψ_H) map. **a** At the DFTr level of theory in vacuo. **b** At the SolDFTr level of theory

(Raymond et al. 1995) also gt(1)–gt(2)–gt(3), has averaged ϕ_H/ψ_H values of 23° to 27°/−23° to −34°. This range of dihedral angles would suggest that the hydroxyl rotamers were nearest the 'c' form, see Fig. 3. For β-cellobiose (Chu and Jeffrey 1968) the corresponding dihedral angles are ∼44° and ∼−12°. The NaI-hydrate of α-cellobiose with the gg′–gg conformations also takes on values of ∼47° and ∼15° (Peralta-Inga et al. 2002). See Table 3 of (Peralta-Inga et al. 2002) for similar structural cellobiose-like results. The NaI-hydrate results suggest that the 'c' form of gg′–gg–c, shown in Fig. 3, would be in agreement with the experimental results. The cyclohexyl derivative of β-D-cellobioside (Yoneda et al. 2008), with mixed hydroxymethyl conformations, A(gg/gt), B(gg/gt), an C(tg/gt) forms, showed average dihedral angles for the central set of ϕ_H/ψ_H ∼ 26°/−34° with the cyclohexyl ends showing considerable variability. As before, these values appear to be in agreement with the in vacuo gt′–gt–c maps of Fig. 7. In all the crystallographic results, one expects that the in vacuo 'c' conformation, would be favored because of the lack of ordered water molecules in the crystalline form, and that appears to be the case.

From coupling constant NMR data in solution, ϕ_H/ψ_H values of 32.2° and −21.1° were found (Cheetham et al. 2003), as were NMR average values of 45° and −38° (Sugiyama et al. 2000), which remained fairly consistent throughout the dimer to hexamer series studied. This small set of data suggests that external conditions as well as preferred conformations of the hydroxymethyl and hydroxyl groups play significant roles in the glycosidic bond conformation. In Fig. 6 the SolDFTr gt′(r)–gt(r) low energy region easily includes both the above results within the ∼0.25 kcal/mol contour, suggesting that the 'r' favored solution structure may be the favored form in a water medium.

References

Andrianov VM, Zhbankov RG, Dashevski VG (1980) A theoretical study of the vibrational spectrum of cellobiose within the framework of the additive model of interatomic interactions. J Struct Chem 21:320–324

Asensio JL, Jimenez-Barbero J (1995) The use of the AMBER force field in conformational analysis of carbohydrate molecules: Determination of the solution conformation of methyl α-lactoside by NMR spectroscopy, assisted by molecular mechanics and dynamics calculations. Biopolymers 35:55–73

Asensio JL, Martin-Pastor M, Jimenez-Barbero J (1997) The use of the MM3* and ESFF force fields in conformational analysis of carbohydrate molecules in solution: the methyl α-lactoside case. J Mol Struct (Theochem) 395–396; 245–270

Bosma WB, Appell M, Willett JL, Momany FA (2006a) Stepwise hydration of cellobiose by DFT methods: 1. Conformational and structural changes brought about by the addition of one to four water molecules. J Mol Struct (THEOCHEM) 776:13–31

Bosma WB, Appell M, Willett JL, Momany FA (2006b) Stepwise hydration of cellobiose by DFT methods: 2. Energy contributions to relative stabilities of cellobiose $(H_2O)_{1-4}$ complexes. J Mol Struct (THEOCHEM) 776:1–11

Cheetham NWH, Dasgupta P, Ball GE (2003) NMR and modeling studies of disaccharide conformation. Carbohydr Res 338:955–962

Chen JY-J, Naidoo KJ (2003) Evaluating intra-molecular hydrogen bond strengths in (1–4) linked disaccharides

from electron density relationships. J Phys Chem B 107:9558–9566

Christensen NJ, Hansen PI, Larsen FH, Folkerman T, Motawia MS, Engelsen SB (2010) A combined nuclear magnetic resonance and molecular dynamics study of the two structural motifs for mixed-linkage β-glucans: methyl β-cellobioside and methyl β-laminarabioside. Carbohydr Res 345:474–486

Chu SSC, Jeffrey GA (1968) The refinement of the crystal structures of β-D-glucose and cellobiose. Acta Cryst B24:830–838

Cocinero EJ, Gamblin DP, Davis BG, Simons JP (2009) The building blocks of cellulose: the intrinsic conformational structures of cellobiose, its epimer, lactose and their singly hydrated complexes. J Am Chem Soc 131:11117–11123

da Silva CO, Nascimento MAC (2004) Ab initio conformational maps for disaccharides in gas phase and aqueous solution. Carbohydr Res 339:113–122

Duus JO, Bock K, Ogawa S (1994) An NMR spectroscopic and conformational study of 12 pseudo-disaccharides (D-glucopyranosyl-5a-carba-D- and–L-gluco- pyranoses). Carbohydr Res 252:1–18

French AD (1988) Rigid- and relaxed-residue conformational analyses of cellobiose using the computer program MM2. Biopolymers 27:1519–1525

French AD, Dowd MK (1993) Exploration of disaccharide conformations by molecular mechanics. J Mol Struct (THEOCHEM) 286:183–201

French AD, Johnson GP (2004) Advanced conformational energy surfaces for cellobiose. Cellulose 11:449–462

French AD, Johnson GP (2006) Quantum mechanics studies of cellobiose conformations. Can J Chem 84:603–612

French AD, Johnson GP (2008) Roles of starting geometries in quantum mechanics studies of cellobiose. Mol Simul 34:365–372

French AD, Johnson GP (2009) Cellulose and the twofold screw axis: modeling and experimental arguments. Cellulose 16:959–973

French AD, Kelterer AM, Johnson GP, Dowd MK, Cramer CJ (2000) Construction and evaluating energy surfaces of crystalline disaccharides. J Mol Graph Model 18:95–107

French AD, Kelterer A-M, Johnson GP, Dowd MK, Cramer CJ (2001) HF/6–31G* energy surfaces for disaccharide analogs. J Comp Chem 22:65–78

Gessler K, Krauss N, Steiner T, Betzel C, Sarko A, Saenger W (1995) β-D-cellotetraose hemihydrate as a structural model for cellulose II. An X-ray diffraction study. J Am Chem Soc 117:11397–11406

Ham JT, Williams DG (1970) The crystal and molecular structure of methyl-β-cellobioside-methanol. Acta Cryst B26:1373–1383

Hamer GK, Balza F, Cyr N, Perlin AS (1978) A conformational study of methyl β-cellobioside-d8 by 13C nuclear magnetic resonance spectroscopy: Dihedral angle dependence of 3JC, H in 13C-O-C-1H arrays. Can J Chem 56:3109–3116

Hardy BJ, Sarko AJ (1993a) Conformational analysis and molecular dynamics simulation of cellobiose and larger cellooligomers. J Comput Chem 14:831–847

Hardy BJ, Sarko AJ (1993b) Molecular dynamics simulation of cellobiose in water. J Comput Chem 14:848–857

Hardy BJ, Gutierrez A, Lesiak K, Seidl E, Widmalm G (1996) Structural analysis of the solution conformation of methyl-4-O-b-D-glucopyranosyl-a-D-glucospyranoside by molecular mechanics and ab initio calculation, stochastic dynamics simulation, and NMR spectroscopy. J Phys Chem 100:9187–9192

Hirotsu K, Shimada A (1974) The crystal and molecular structure of β-lactose. Bull Chem Soc Jpn 47:1872–1879

Homans SW (1993) Conformation and dynamics of oligosaccharides in solution. Glycobiology 3:551–555

Horii F, Hirai A, Kitamaru R (1982) Solid-state high-resolution ^{13}C-NMR studies of regenerated cellulose samples with different crystallinities. Polym Bull 8:163–170

Horii F, Hirai A, Kitamaru R (1983) Solid-state ^{13}C-NMR study of conformations of oligosaccharides and cellulose. Polym Bull 10:357–361

Hyperchem v8.0.2 (2007) Hypercube, Inc. 115 NW 4th Street, Gainesville, FL, 32602. USA

Johnson GP, Petersen L, French AD, Reilly PJ (2009) Twisting of glycosidic bonds by hydrolases. Carbohydr Res 344:2157–2166

Kirschner KN, Woods RJ (2001) Solvent interactions determine carbohydrate conformation. Proc Natl Acad Sci 11:10541–10545

Klamt A, Schüürmann GJ (1993) COSMO-A new approach to dielectric screening in solvents with explicit expressions for the screening energy and its gradient. J Chem Soc Perkin Tran II:799–805

Korolik EV, Ivanova NV, Kolosova TE, Zhbankov RG (1985) Investigation of the IR spectra of cellobiose and *O*-deuterated cellobiose at the temperature of liquid helium. J Appl Spectrosc 42:551–553

Larsson EA, Staaf M, Soderman P, Hoog C, Widmalm G (2004) Determination of the conformational flexibility of methyl α-cellobioside in solution by NMR spectroscopy and molecular simulations. J Phys Chem A 108: 3932–3937

Leung F, Chanzy HD, Perez S, Marchessault RH (1976) Crystal structure of β-D-acetyl cellobiose, $C_{28}H_{38}O_{19}$. Can J Chem 54:1365–1371

Mackie ID, Rohrling J, Gould RO, Pauli J, Jager C, Walkinshaw M, Potthast A, Rosenau T, Kosma P (2002) Crystal and molecular structure of methyl 4-*O*-methyl-β-D-glucopyranosyl-(1 → 3)-β-D-glucopyranoside. Carbohydr Res 337:161–166

Mendonca S, Johnson GP, French AD, Laine RA (2002) Conformational analyses of native and permethylated disaccharides. J Phys Chem A 106:4115–4124

Momany FA, Schnupf U (2011) DFTMD studies of b-cellobiose: conformational preference using implicit solvent. Carbohydr Res 340:619–630

Olsson U, Serianni AS, Stenutz R (2008) Conformational analysis of β-glycosidic linkages in ^{13}C-labeled glucobioside using inter-residue scalar coupling constants. J Phys Chem B112:4447–4453

Origin v8.0 (2009) OriginLab Corporation, Northampton, MA

Peralta-Inga Z, Johnson GP, Dowd MK, Rendleman JA, Stevens ED, French AD (2002) The crystal structure of the α-cellobiose 2 NaI·2 H_2O complex in the context of related

structures and conformational analysis. Carbohydr Res 337:851–861

Pereira CS, Kony D, Baron R, Muller M, van Gunsteren WF, Hunenberger PH (2006) Conformational and dynamical properties of disaccharides in water: a molecular dynamics study. Biophys J 90:4337–4344

Peters T, Meyer B, Stuike-Prill R, Somorjai R, Brisson J-R (1993) A Monte Carlo method for conformational analysis of saccharides. Carbohydr Res 238:49–73

PQS, Ab Initio Program Package v3.3 (2009) Parallel Quantum Solutions, 2013 Green Acres, Suite E, Fayetteville, AR 72703, USA

Raymond S, Henrissat B, Qui DT, Kvick A, Chanzy H (1995) The crystal structure of methyl β-cellotrioside monohydrate 0.25 ethanolate and its relationship to cellulose II. Carbohydr Res 277:209–229

Rencurosi A, Rohrling J, Pauli J, Potthast A, Jager C, Perez S, Kosma P, Imberty A (2002) Polymorphism in the crystal structure of the cellulose fragment analogue methyl 4-*O*-methyl-β-D-glucopyranosyl-(1–4)-β-D-glucopyranoside. Angew Chem Int Ed 41:4277–4281

Schnupf U, Willett JL, Bosma WB, Momany FA (2007) DFT studies of the disaccharide, α-maltose: relaxed isopotential maps. Carbohydr Res 342:2270–2285

Schnupf U, Willett JL, Momany FA (2011) 27 ps DFT molecular dynamics simulation of a-maltose: a reduced basis set study. J Comput Chem 31:2087–2097

Sergeyev I, Moyna G (2005) Determination of the three-dimensional structure of oligosaccharides in the solid state from experimental 13C NMR data and ab initio chemical shift surfaces. Carbohydr Res 340:1165–1174

Shen T, Langan P, French AD, Johnson GP, Gnanakaran S (2009) Conformational flexibility of soluble cellulose oligomers: chain length and temperature dependence. J Am Chem Soc 131:14786–14794

Sivchik VV, Zhbankov RG (1977) Theoretical investigation of the vibrational spectrum of cellobiose. Translated from Zhurnal Prikladnoi Spektroskopii 27:853–859

Stortz CA, Cerezo AS (2002) Disaccharide conformational maps: 3D contours or 2D plots? Carbohydr Res 337:1861–1871

Stortz CA, Cerezo AS (2003) Depicting the MM3 potential energy surfaces of trisaccharides by single contour maps: application to β-cellotriose and α-maltotriose. Carbohydr Res 338:95–107

Stortz CA, French AD (2008) Disaccharide conformational maps: adiabaticity in analogues with variable ring shapes. Mol Simul 34:373–389

Stortz CA, Johnson GP, French AD, Csonka GI (2009) Comparison of different force fields for the study of disaccharides. Carbohydr Res 344:2217–2228

Strati GL, Willett JL, Momany FA (2002a) Ab initio computational study of β-cellobiose conformers using B3LYP/6–311++G**. Carbohydr Res 337:1833–1849

Strati GL, Willett JL, Momany FA (2002b) A DFT/ab initio study of hydrogen bonding and conformational preference in model cellobiose analogs using B3LYP/6–311++G**. Carbohydr Res 337:1851–1859

Sugiyama H, Hisamichi K, Usui T, Sakai K, Ishiyama J-i (2000) A study of the conformation of β-1, 4-linked glucose oligomers, cellobiose to cellohexaose, in solution. J Mol Struct (THEOCHEM) 556:173–177

Suzuki S, Horii F, Kurosu H (2009) Theoretical investigations of ^{13}C chemical shifts in glucose, cellobiose, and native cellulose by quantum chemistry calculations. J Mol Struct (THEOCHEM) 921:219–226

Tvaroska I (1984) Theoretical studies on the conformation of saccharides. VIII. Solvent effect on the stability of β-cellobiose conformers. Biopolymers 23:1951–1960

Tvaroska I, Taravel FR (1992) One-bond carbon-proton coupling constants: angular dependence in β-linked oligosaccharides. J Biomol NMR 2:421–430

Umemura M, Hayashi S, Nakagawa T, Yamanaka S, Urakawa H, Kajiwara K (2003a) Structure of water molecules in aqueous maltose and cellobiose solutions using molecular dynamics simulation. I. Statics. J Mol Struct (THEOCHEM) 624:129–144

Umemura M, Hayashi S, Nakagawa T, Urakawa H, Kajiwara K (2003b) Structure of water molecules in aqueous maltose and cellobiose solutions using molecular dynamics simulation. II. Dynamics. J Mol Struct (THEOCHEM) 636:215–228

Umemura M, Yuguchi Y, Hirotsu T (2005) Hydration at glycosidic linkages of malto- and cello-oligosaccharides in aqueous solution from molecular dynamics simulation: effect of conformational flexibility. J Mol Struct (THEOCHEM) 730:1–8

Vietor RJ, Mazeau K, Lakin M, Perez S (2000) A priori crystal structure prediction of native celluloses. Biopolymers 54:342–354

Wacowich-Sgarbi SA, Ling CC, Otter A, Bundle DR (2001) A tethered disaccharide trapped as its anti-conformer calibrates the Karplus relationship for 3JC, H coupling constants. J Am Chem Soc 123:4362–4363

Yoneda Y, Mereiter K, Jaeger C, Brecker L, Kosma P, Rosenau T, French A (2008) van der Waals versus hydrogen-bonding forces in a crystalline analog of cellotetraose: cyclohexyl 4′-*O*-cyclohexyl β-D-cellobioside cyclohexane solvent. J Am Chem Soc 130:16678–16690

York WS, Yi X (2004) CONDORR-CONstrained dynamics of rigid residues: a molecular dynamics program for constrained molecules. J Mol Model 10:271–289

Zhang W, Zhao W, Carmichael H, Serianni AS (2009) An NMR investigation of putative inter-residue H-bonding in methyl α-cellobioside in solution. Carbohydr Res 344:1582–1587